A Experiment details

We conducted all experiments in the paper using three random seeds (0, 1, 2) and reported the average accuracies and their corresponding standard deviations. The experiments were performed on NVIDIA GeForce RTX 3090 and NVIDIA TITAN RTX GPUs. For a single execution of SoTTA, the test-time adaptation phase consumed 1 minutes for CIFAR10-C/CIFAR100-C and 10 minutes for ImageNet-C.

A.1 Baseline details

In this study, we utilized the official implementations of the baseline methods. To ensure consistency, we adopted the reported best hyperparameters documented in the respective papers or source code repositories. Furthermore, we present supplementary information regarding the implementation specifics of the baseline methods and provide a comprehensive overview of our experimental setup, including detailed descriptions of the employed hyperparameters.

SoTTA (Ours). We used ADAM optimizer [14], with a BN momentum of $m = 0.2$, and learning rate of $l = 0.001$ with a single adaptation epoch. We set the HUS size to 64 and the confidence threshold C_0 to 0.99 for CIFAR10-C (10 classes), 0.66 for CIFAR100-C (100 classes), and 0.33 for ImageNet-C (1,000 classes). We set entropy-sharpness L2-norm constraint $\rho = 0.5$ following the suggestion [4].

PL. For PL [17], we only updated the BN layers following the previous studies [38, 39]. We set the learning rate as $LR = 0.001$ as the same as TENT [38].

TENT. For TENT [38], we set the learning rate as $LR = 0.001$ for CIFAR10-C and $LR = 0.00025$ for ImageNet-C, following the guidance provided in the original paper. We referred to the official code[3] for implementations.

LAME. LAME [1] relies on an affinity matrix and incorporates hyperparameters associated with it. We followed the hyperparameter selection specified by the authors in their paper and referred to their official code[4] for implementation details. Specifically, we employed the kNN affinity matrix with a value of k set to 5.

CoTTA. CoTTA [39] incorporates three hyperparameters: the augmentation confidence threshold p_{th}, restoration factor p, and exponential moving average (EMA) factor m. To ensure consistency, we adopted the hyperparameter values recommended by the authors. Specifically, we set the restoration factor to $p = 0.01$ and the EMA factor to $\alpha = 0.999$. For the augmentation confidence threshold, the authors provide a guideline for its selection, suggesting using the 5% quantile of the softmax predictions' confidence on the source domains. We followed this guideline, which results in $p_{th} = 0.92$ for CIFAR10-C, $p_{th} = 0.72$ for CIFAR100-C, and $p_{th} = 0.1$ for ImageNet-C. We referred to the official code[5] for implementing CoTTA.

EATA. For EATA [28], we followed the settings from the original paper. We set $LR = 0.005/0.005/0.00025$ for CIFAR10-C/CIFAR100-C/ImageNet-C, entropy constant $E_0 = 0.4 \times \ln|\mathcal{Y}|$ where $|\mathcal{Y}|$ is number of classes. We set cosine sample similarity threshold $\epsilon = 0.4/0.4/0.05$, trade-off parameter $\beta = 1/1/2,000$, the moving average factor $\alpha = 0.1$. We utilized 2,000 samples for calculating Fisher importance as suggested. We referred to the official code[6] for implementing EATA.

SAR. SAR [29] aims to adapt to diverse batch sizes, and we chose a typical batch size of 64 for a fair comparison. We followed the learning rate as $LR = 0.00025$, sharpness threshold $\rho = 0.5$, and entropy threshold $E_0 = 0.4 \times \ln|\mathcal{Y}|$ where $|\mathcal{Y}|$ is the total number of classes, as suggested in the original paper. Finally, we froze the top layer (layer4 for ResNet18) as the original paper, and SoTTA also follows this implementation. We referred to the original code[7] for implementing SAR.

[3] https://github.com/DequanWang/tent
[4] https://github.com/fiveai/LAME
[5] https://github.com/qinenergy/cotta
[6] https://github.com/mr-eggplant/EATA
[7] https://github.com/mr-eggplant/SAR

RoTTA. RoTTA [44] uses Adam Optimizer by setting learning rate as $LR = 0.001$ and $\beta = 0.9$. We followed the authors' hyperparameters selection from the paper, including BN-statistic exponential moving average updating rate as $\alpha = 0.05$, the Teacher model's exponential moving average updating rate as $\nu = 0.001$, timeliness parameter as $\lambda_t = 1.0$, and uncertainty parameter as $\lambda_u = 1.0$. We referred to the original code[8] for implementing RoTTA.

A.2 Target dataset details

CIFAR10-C/CIFAR100-C. CIFAR10-C/CIFAR100-C [9] serves as a widely adopted benchmark for evaluating the robustness of models against corruptions [27, 36, 38, 39]. Both datasets consist of 50,000 training samples and 10,000 test samples, categorized into 10/100 classes. To assess the robustness of models, datasets introduce 15 types of corruptions to the test data, including Gaussian Noise, Shot Noise, Impulse Noise, Defocus Blur, Frosted Glass Blur, Motion Blur, Zoom Blur, Snow, Frost, Fog, Brightness, Contrast, Elastic Transformation, Pixelate, and JPEG Compression. For our experiments, we adopt the highest severity level of corruption, level 5, in line with previous studies [27, 36, 38, 39]. Consequently, the datasets consist of 150,000 corrupted test samples. To train our models, we employ the ResNet18 [8] architecture as the backbone network. The model is trained on the clean training data to generate the source models. We utilize stochastic gradient descent with a momentum of 0.9 and cosine annealing learning rate scheduling [22] for 200 epochs. The initial learning rate is set to 0.1, and a batch size 128 is used during training.

ImageNet-C. ImageNet-C is another widely adopted benchmark for evaluating the robustness of models against corruptions [1, 27, 36, 38, 39]. The ImageNet dataset [3] consists of 1,281,167 training samples and 50,000 test samples. Similar to CIFAR10-C, ImageNet-C applies the same 15 types of corruptions, resulting in 750,000 corrupted test samples. We utilize the highest severity level of corruption, equivalent to CIFAR10-C. For our experiments, we employ a pre-trained ResNet18 [8] model from the TorchVision library [23], which is pre-trained on the ImageNet dataset [3] and is widely used as a backbone for various computer vision tasks.

A.3 Noisy dataset details

CIFAR100 (Near). CIFAR100 [15] consists of 50,000/10,000 training/test data with 100 classes. We utilized training data without any corruption. We undersampled the dataset to 10,000 for the CIFAR10-C and CIFAR100-C target cases by randomly removing samples and used the entire training set (50,000) for the ImageNet-C target case.

ImageNet (Near). ImageNet [3] consists of 1,281,167/50,000 training/test data with 1,000 classes. We utilized test data without any corruption. We undersampled the dataset to 10,000 for the CIFAR100-C target case by randomly removing samples.

MNIST (Far). MNIST [16] contains 60,000/10,000 training/test data with 10 classes. We utilized test data without any corruption. We used the entire test set for the CIFAR10-C/CIFAR100-C target case, and oversampled the dataset by randomly resampling, which results in 50,000 samples that is equivalent to the size of each ImageNet-C target data.

Attack. We implemented the modified indiscriminate distribution invading attack (DIA) [40]. First, we duplicated the entire set of target samples and treated them as malicious samples. Subsequently, we randomly shuffled these duplicated samples within the original target sample set. During the adaptation phase, we injected perturbations into the malicious samples to increase the overall error rate on benign samples within the same batch. As a result, we perturbed 10,000 samples (CIFAR10-C/CIFAR100-C) and 50,000 samples (ImageNet-C) to serve as attack samples. For CIFAR10-C/CIFAR100-C, we used hyperparameters of maximum perturbation constraint $\epsilon = 0.1$, attack learning rate $\alpha = 1/255$, and attacking steps $N = 10$. For ImageNet-C, we used hyperparameters of maximum perturbation constraint $\epsilon = 0.2$, attack learning rate $\alpha = 1/255$, and attacking steps $N = 1$.

Uniform random noise (Noise). We generated a uniform random valued image in the scaled RGB range $[0, 1]$, with the same height and width as the corresponding target dataset. We generated the same amount of noise samples as each target dataset.

[8] https://github.com/BIT-DA/RoTTA

B Result details

Table 5: Classification accuracy (%) and their corresponding standard deviations on CIFAR10-C for 15 types of corruptions under five scenarios. **Bold** numbers are the highest accuracy. Averaged over three different random seeds.

		Noise			Blur				Weather				Digital				
	Method	Gau.	Shot	Imp.	Def.	Gla.	Mot.	Zoom	Snow	Fro.	Fog	Brit.	Cont.	Elas.	Pix.	JPEG	Avg.
Benign	Source	26.0 ± 3.3	33.2 ± 3.5	24.7 ± 4.2	56.7 ± 2.7	52.0 ± 2.7	67.4 ± 1.2	64.8 ± 2.6	78.0 ± 0.4	67.0 ± 2.5	74.1 ± 0.8	91.5 ± 0.3	33.9 ± 1.8	76.6 ± 0.7	46.4 ± 0.6	73.2 ± 0.8	57.7 ± 1.0
	BN Stats [27]	67.0 ± 0.5	69.0 ± 0.8	60.4 ± 0.9	87.8 ± 0.2	65.6 ± 0.7	86.3 ± 0.1	87.4 ± 0.4	81.6 ± 0.4	80.3 ± 0.5	85.4 ± 0.6	90.7 ± 0.2	86.9 ± 0.4	76.7 ± 0.2	79.3 ± 0.0	71.9 ± 0.6	78.4 ± 0.3
	PL [17]	71.1 ± 1.2	72.9 ± 0.6	62.2 ± 1.3	86.9 ± 0.0	64.4 ± 0.4	85.3 ± 1.2	86.6 ± 0.9	80.8 ± 1.0	78.8 ± 1.8	84.9 ± 0.3	89.6 ± 1.0	84.0 ± 0.2	76.2 ± 0.6	80.0 ± 0.7	73.1 ± 1.4	78.5 ± 0.3
	TENT [38]	74.5 ± 0.7	77.6 ± 0.8	66.6 ± 1.3	88.2 ± 0.3	66.2 ± 2.0	86.9 ± 0.8	88.8 ± 0.4	83.7 ± 0.5	81.3 ± 1.3	86.0 ± 1.5	91.1 ± 0.4	86.9 ± 0.6	77.9 ± 0.3	82.7 ± 0.9	76.7 ± 1.4	81.0 ± 0.4
	LAME [1]	21.8 ± 3.6	29.2 ± 4.0	19.7 ± 4.7	53.3 ± 1.6	52.1 ± 3.7	65.9 ± 0.3	62.5 ± 1.4	79.2 ± 0.7	69.3 ± 4.4	73.1 ± 1.7	90.1 ± 0.3	28.0 ± 1.1	75.7 ± 0.7	43.8 ± 1.1	74.1 ± 0.9	55.9 ± 0.5
	CoTTA [39]	**76.9 ± 0.6**	**78.6 ± 0.1**	**72.3 ± 0.2**	88.2 ± 0.5	**70.9 ± 1.0**	86.8 ± 0.2	88.1 ± 0.5	83.4 ± 0.3	83.4 ± 0.5	86.1 ± 0.5	91.2 ± 0.2	84.9 ± 0.2	79.2 ± 0.5	83.0 ± 0.3	**79.9 ± 0.6**	82.2 ± 0.2
	EATA [28]	76.0 ± 0.8	78.2 ± 0.8	68.2 ± 0.7	88.4 ± 0.2	70.1 ± 1.9	87.4 ± 0.5	88.4 ± 0.1	84.5 ± 0.3	**85.0 ± 0.3**	88.0 ± 0.2	91.5 ± 0.3	**89.9 ± 0.6**	77.8 ± 0.5	**84.8 ± 0.5**	78.4 ± 1.2	**82.4 ± 0.2**
	SAR [29]	68.3 ± 1.2	69.7 ± 1	58.9 ± 6.9	87.8 ± 0.2	62.9 ± 5.3	86.3 ± 0.1	87.4 ± 0.4	81.6 ± 0.4	80.3 ± 0.5	85.4 ± 0.6	90.7 ± 0.2	86.9 ± 0.5	76.7 ± 0.2	79.3 ± 0	72.0 ± 0.5	78.3 ± 0.7
	RoTTA [44]	65.2 ± 0.8	67.4 ± 1.1	58.3 ± 0.9	87.2 ± 0.2	64.4 ± 1.2	85.8 ± 0.5	87.3 ± 0.5	81.2 ± 1	76.9 ± 1	85.3 ± 0.6	90.7 ± 0.5	57.2 ± 2.9	76.5 ± 0.5	77.7 ± 0.4	71.6 ± 0.9	75.5 ± 0.7
	SoTTA	75.0 ± 1.1	77.5 ± 0.6	68.8 ± 0.7	**88.8 ± 0.4**	70.7 ± 1.2	**87.5 ± 0.5**	**89.0 ± 0.5**	**85.4 ± 0.3**	84.0 ± 0.7	**88.2 ± 0.2**	**91.9 ± 0.1**	83.9 ± 1.5	**79.8 ± 0.4**	83.9 ± 0.5	78.3 ± 0.7	82.2 ± 0.3
Near	Source	26.0 ± 3.3	33.2 ± 3.5	24.7 ± 4.2	56.7 ± 2.7	52.0 ± 2.7	67.4 ± 1.2	64.8 ± 2.6	78.0 ± 0.4	67.0 ± 2.5	74.1 ± 0.8	91.5 ± 0.3	33.9 ± 1.8	76.6 ± 0.7	46.4 ± 0.6	73.2 ± 0.8	57.7 ± 1.0
	BN Stats [27]	64.9 ± 0.8	66.3 ± 0.9	58.2 ± 0.7	84.1 ± 0.5	62.7 ± 0.6	84.2 ± 0.4	85.0 ± 0.2	83.1 ± 0.6	82.5 ± 0.5	85.5 ± 0.5	92.4 ± 0.1	85.3 ± 0.2	76.5 ± 0.6	67.4 ± 0.3	70.3 ± 1.0	76.6 ± 0.4
	PL [17]	63.2 ± 1.0	63.5 ± 3.4	51.7 ± 4.4	81.6 ± 1.0	58.4 ± 1.5	78.4 ± 1.6	83.3 ± 0.6	79.2 ± 0.5	79.7 ± 2.1	80.3 ± 1.9	89.2 ± 1.1	79.5 ± 0.1	73.1 ± 1.6	70.9 ± 0.6	69.3 ± 1.7	73.4 ± 0.2
	TENT [38]	64.7 ± 3.6	64.7 ± 5.4	50.2 ± 4.9	81.3 ± 2.3	59.6 ± 2.9	80.8 ± 1.1	83.8 ± 1.0	79.6 ± 1.1	78.3 ± 2.7	80.0 ± 3.8	88.6 ± 1.0	83.7 ± 1.4	73.5 ± 1.0	74.3 ± 0.5	71.1 ± 2.8	74.3 ± 0.9
	LAME [1]	24.3 ± 3.0	31.6 ± 3.3	19.9 ± 4.3	53.9 ± 1.4	53.2 ± 3.6	65.9 ± 0.7	62.5 ± 1.2	79.0 ± 0.4	69.5 ± 3.8	73.1 ± 1.5	90.1 ± 0.2	28.4 ± 1.1	75.0 ± 0.7	44.8 ± 1.0	74.2 ± 1.1	56.4 ± 0.6
	CoTTA [39]	72.7 ± 0.2	74.3 ± 0.7	66.0 ± 0.1	82.6 ± 0.6	**67.6 ± 0.9**	81.8 ± 0.5	84.1 ± 0.4	84.1 ± 0.8	**85.5 ± 0.3**	82.5 ± 1.1	91.1 ± 0.3	69.9 ± 0.5	78.1 ± 1.0	76.1 ± 0.5	**79.3 ± 0.7**	78.4 ± 0.4
	EATA [28]	51.5 ± 3.4	50.3 ± 2.4	40.1 ± 2.2	70.4 ± 5.6	45.8 ± 2.4	72.8 ± 0.9	77.2 ± 1.4	66.8 ± 2.0	67.4 ± 5.0	74.4 ± 1.2	83.9 ± 1.2	68.2 ± 7.5	60.2 ± 1.8	67.3 ± 2.0	62.1 ± 5.4	63.9 ± 0.4
	SAR [29]	59.0 ± 15.4	60.9 ± 14.3	52.8 ± 14.4	78.2 ± 10.0	55.4 ± 14.7	83.7 ± 0.7	81.8 ± 5.7	78.8 ± 7.2	78.6 ± 6.7	85.5 ± 0.5	**92.4 ± 0.1**	85.3 ± 0.1	66.6 ± 17.8	64.0 ± 12.2	63.8 ± 14.4	72.4 ± 8.8
	RoTTA [44]	66.3 ± 0.7	68.3 ± 1.3	59.4 ± 0.7	86.0 ± 0.4	63.2 ± 0.7	85.4 ± 0.3	87.0 ± 0.4	83.5 ± 0.8	82.8 ± 0.7	86.4 ± 0.5	**92.4 ± 0.3**	84.8 ± 1.4	77.1 ± 0.8	71.6 ± 0.4	71.6 ± 0.6	77.7 ± 0.6
	SoTTA	**74.3 ± 1.4**	**76.7 ± 0.9**	**66.5 ± 2.2**	**87.5 ± 0.1**	66.9 ± 0.8	**86.4 ± 0.6**	**87.8 ± 0.5**	**84.4 ± 0.6**	83.8 ± 0.2	**87.2 ± 0.5**	91.3 ± 0.2	**88.4 ± 0.7**	**78.7 ± 1.1**	**82.4 ± 0.5**	78.0 ± 0.6	**81.4 ± 0.5**
Far	Source	26.0 ± 3.3	33.2 ± 3.5	24.7 ± 4.2	56.7 ± 2.7	52.0 ± 2.7	67.4 ± 1.2	64.8 ± 2.6	78.0 ± 0.4	67.0 ± 2.5	74.1 ± 0.8	91.5 ± 0.3	33.9 ± 1.8	76.6 ± 0.7	46.4 ± 0.6	73.2 ± 0.8	57.7 ± 1.0
	BN Stats [27]	62.7 ± 1.3	66.1 ± 1.4	56.0 ± 0.9	86.5 ± 0.2	60.7 ± 0.7	84.2 ± 0.8	87.2 ± 0.1	79.8 ± 0.4	78.4 ± 0.6	85.7 ± 0.2	89.9 ± 0.0	80.2 ± 1.0	75.5 ± 0.6	69.8 ± 1.0	65.0 ± 0.1	75.2 ± 0.3
	PL [17]	55.2 ± 2.9	54.1 ± 5.2	48.3 ± 5.2	83.2 ± 0.8	49.3 ± 4.4	80.0 ± 2.4	83.0 ± 1.9	76.8 ± 1.2	73.3 ± 2.8	80.6 ± 1.9	87.6 ± 1.4	74.6 ± 2.0	70.5 ± 2.7	66.8 ± 5.9	63.6 ± 2.6	69.8 ± 1.5
	TENT [38]	51.6 ± 8.6	57.4 ± 6.2	43.7 ± 11.4	84.8 ± 0.8	43.5 ± 7.5	83.3 ± 0.8	85.3 ± 0.6	80.4 ± 1.1	73.1 ± 3.5	83.5 ± 0.4	88.9 ± 0.4	80.8 ± 7.5	73.5 ± 1.7	72.2 ± 2.4	66.7 ± 4.3	71.2 ± 1.0
	LAME [1]	22.8 ± 3.4	29.6 ± 3.7	19.3 ± 4.2	53.2 ± 1.6	50.4 ± 3.7	64.6 ± 0.8	60.7 ± 1.2	79.1 ± 0.7	67.9 ± 4.0	72.8 ± 1.5	90.1 ± 0.2	28.1 ± 1.1	74.7 ± 0.8	44.4 ± 0.7	74.3 ± 1.0	55.5 ± 0.4
	CoTTA [39]	67.4 ± 1.9	71.1 ± 1.0	59.4 ± 2.7	83.3 ± 0.5	61.2 ± 0.6	82.3 ± 0.9	84.3 ± 0.3	80.4 ± 1.2	80.4 ± 1.5	83.8 ± 1.3	87.2 ± 1.4	58.0 ± 4.7	76.0 ± 0.4	70.3 ± 3.5	72.9 ± 2.7	74.5 ± 1.2
	EATA [28]	40.0 ± 2.3	46.4 ± 3.9	34.9 ± 0.9	73.5 ± 0.3	35.2 ± 2.9	59.3 ± 2.8	76.4 ± 0.7	61.1 ± 3.0	59.5 ± 2.9	68.4 ± 7.1	85.2 ± 2.1	55.2 ± 9.0	46.5 ± 1.2	53.5 ± 5.1	49.0 ± 5.5	56.3 ± 0.5
	SAR [29]	60.3 ± 7.7	62.6 ± 7.9	50.9 ± 9.8	86.5 ± 0.2	55.4 ± 9.6	84.3 ± 0.7	87.2 ± 0.1	79.8 ± 0.3	78.3 ± 0.5	85.7 ± 0.2	89.9 ± 0.1	80.2 ± 0.9	70.1 ± 10.1	67.8 ± 6.2	60.9 ± 9.5	73.3 ± 3.9
	RoTTA [44]	67.3 ± 0.5	69.8 ± 1.0	61.1 ± 1.9	88.1 ± 0.4	66.0 ± 0.9	86.6 ± 0.5	88.0 ± 0.6	82.0 ± 1.1	78.8 ± 1.4	86.2 ± 0.6	91.2 ± 0.4	61.7 ± 9.5	77.5 ± 0.8	79.6 ± 1.0	73.0 ± 1.0	77.1 ± 1.1
	SoTTA	**73.3 ± 1.2**	**76.3 ± 1.9**	**66.3 ± 2.5**	**88.5 ± 0.6**	**68.3 ± 2.3**	**86.8 ± 0.7**	**88.3 ± 0.2**	**84.1 ± 1.0**	**84.2 ± 0.6**	**87.2 ± 0.4**	**92.0 ± 0.4**	**89.0 ± 1.1**	**77.8 ± 1.8**	**83.8 ± 0.9**	**77.8 ± 1.2**	**81.6 ± 0.6**
Attack	Source	26.0 ± 3.3	33.2 ± 3.5	24.7 ± 4.2	56.7 ± 2.7	52.0 ± 2.7	67.4 ± 1.2	64.8 ± 2.6	78.0 ± 0.4	67.0 ± 2.5	74.1 ± 0.8	91.5 ± 0.3	33.9 ± 1.8	76.6 ± 0.7	46.4 ± 0.6	73.2 ± 0.8	57.7 ± 1.0
	BN Stats [27]	44.5 ± 1.3	46.8 ± 1.5	39.8 ± 1.1	63.3 ± 1.2	42.1 ± 1.7	63.5 ± 1.7	62.5 ± 1.2	62.3 ± 1.7	59.3 ± 1.7	62.1 ± 1.5	75.4 ± 1.0	65.1 ± 1.4	50.6 ± 1.3	53.9 ± 1.6	46.9 ± 1.9	55.9 ± 1.4
	PL [17]	59.1 ± 0.9	61.4 ± 1.5	53.1 ± 2.0	73.1 ± 0.9	51.9 ± 2.0	71.7 ± 1.8	72.3 ± 1.1	71.3 ± 1.7	69.1 ± 1.7	69.8 ± 0.8	81.5 ± 0.9	72.1 ± 0.7	60.9 ± 1.8	67.4 ± 1.2	60.1 ± 1.4	66.3 ± 1.3
	TENT [38]	62.9 ± 0.6	65.2 ± 0.3	56.7 ± 1.1	74.8 ± 1.0	54.5 ± 2.0	73.4 ± 0.8	75.2 ± 0.9	73.8 ± 0.6	71.8 ± 1.8	72.1 ± 0.6	83.0 ± 0.7	73.7 ± 0.5	63.1 ± 1.3	70.0 ± 1.0	64.0 ± 1.4	68.9 ± 0.9
	LAME [1]	21.0 ± 3.5	28.0 ± 4.1	17.3 ± 4.3	52.7 ± 1.9	52.9 ± 3.6	65.9 ± 0.5	62.0 ± 1.2	79.3 ± 0.6	70.4 ± 4.5	73.9 ± 1.6	90.3 ± 0.2	28.4 ± 1.0	75.6 ± 0.7	44.2 ± 1.0	74.2 ± 1.1	55.9 ± 0.5
	CoTTA [39]	53.1 ± 1.6	57.0 ± 1.2	49.7 ± 1.8	67.9 ± 0.7	55.9 ± 2.4	69.7 ± 1.6	71.3 ± 0.6	74.3 ± 1.8	69.5 ± 1.9	68.1 ± 2.0	84.9 ± 0.4	47.0 ± 2.9	68.6 ± 1.9	62.3 ± 1.6	71.6 ± 1.3	69.5 ± 1.5
	EATA [28]	66.6 ± 0.4	68.7 ± 0.5	57.9 ± 0.5	75.2 ± 0.7	57.2 ± 0.8	74.7 ± 1.0	75.5 ± 0.9	75.1 ± 1.0	73.5 ± 0.8	73.8 ± 0.5	83.5 ± 0.6	76.0 ± 0.9	64.3 ± 1.0	73.5 ± 0.6	67.8 ± 1.1	70.9 ± 0.6
	SAR [29]	46.1 ± 3.9	48.1 ± 3.5	40.3 ± 1.7	63.3 ± 1.2	42.2 ± 1.6	63.5 ± 1.8	62.5 ± 1.2	62.3 ± 1.7	59.3 ± 1.7	62.1 ± 1.5	75.4 ± 1.0	65.1 ± 1.4	50.6 ± 1.2	53.9 ± 1.7	47.6 ± 2.9	56.2 ± 1.8
	RoTTA [44]	69.7 ± 0.7	71.8 ± 1.0	62.9 ± 1.0	88.6 ± 0.3	67.8 ± 0.7	87.4 ± 0.2	88.7 ± 0.6	83.2 ± 0.7	80.1 ± 0.8	87.1 ± 0.3	91.8 ± 0.3	63.5 ± 3.7	78.4 ± 0.8	80.6 ± 0.2	74.1 ± 0.7	78.4 ± 0.7
	SoTTA	**78.2 ± 0.3**	**80.8 ± 0.1**	**72.3 ± 0.8**	**90.1 ± 0.2**	**73.6 ± 0.9**	**89.2 ± 0.4**	**90.3 ± 0.5**	**87.4 ± 0.5**	**86.2 ± 0.6**	**89.3 ± 0.6**	**92.9 ± 0.1**	**87.8 ± 0.7**	**81.3 ± 0.8**	**86.6 ± 0.3**	**81.0 ± 0.3**	**84.5 ± 0.2**
Noise	Source	26.0 ± 3.3	33.2 ± 3.5	24.7 ± 4.2	56.7 ± 2.7	52.0 ± 2.7	67.4 ± 1.2	64.8 ± 2.6	78.0 ± 0.4	67.0 ± 2.5	74.1 ± 0.8	**91.5 ± 0.3**	33.9 ± 1.8	76.6 ± 0.7	46.4 ± 0.6	73.2 ± 0.8	57.7 ± 1.0
	BN Stats [27]	51.7 ± 0.3	53.9 ± 0.6	45.5 ± 0.7	52.7 ± 2.0	41.5 ± 1.7	51.0 ± 0.7	55.1 ± 1.5	62.8 ± 0.7	63.8 ± 0.2	53.8 ± 0.6	76.9 ± 0.3	55.8 ± 2.5	46.8 ± 1.8	54.8 ± 0.7	56.4 ± 1.0	54.8 ± 0.8
	PL [17]	47.6 ± 9.9	52.7 ± 2.4	44.7 ± 4.3	48.9 ± 12.6	36.1 ± 5.1	49.4 ± 1.8	54.1 ± 2.9	61.9 ± 2.4	56.5 ± 4.4	50.9 ± 1.3	77.1 ± 3.7	45.2 ± 4.8	43.1 ± 4.5	49.4 ± 5.6	59.5 ± 4.7	51.8 ± 0.9
	TENT [38]	54.0 ± 6.7	57.1 ± 5.6	36.7 ± 9.1	48.9 ± 6.8	28.3 ± 4.5	50.5 ± 3.1	51.0 ± 5.0	64.0 ± 4.1	64.7 ± 5.2	49.5 ± 1.9	80.5 ± 1.4	43.7 ± 3.0	38.4 ± 2.2	56.7 ± 6.4	57.0 ± 4.5	52.1 ± 0.4
	LAME [1]	21.8 ± 3.5	28.6 ± 3.7	18.5 ± 3.1	51.6 ± 2.3	50.8 ± 3.6	64.3 ± 0.2	60.9 ± 1.8	78.4 ± 0.5	67.3 ± 3.8	71.7 ± 1.2	90.5 ± 0.2	27.0 ± 1.2	75.1 ± 0.7	43.0 ± 0.9	73.4 ± 1.0	54.9 ± 0.6
	CoTTA [39]	60.4 ± 2.1	60.3 ± 3.5	52.4 ± 1.6	47.3 ± 3.0	41.6 ± 0.4	44.1 ± 2.7	52.0 ± 4.7	62.7 ± 0.6	66.6 ± 0.8	47.7 ± 2.4	79.0 ± 1.7	44.7 ± 1.1	42.8 ± 4.3	60.2 ± 0.5	60.2 ± 1.0	54.8 ± 1.3
	EATA [28]	42.2 ± 1.1	41.0 ± 1.1	33.2 ± 5.9	32.7 ± 5.1	25.0 ± 1.5	27.9 ± 2.1	34.3 ± 5.4	40.8 ± 2.7	42.6 ± 6.5	31.6 ± 11.5	61.5 ± 5.7	20.3 ± 2.2	27.5 ± 4.1	35.8 ± 4.5	43.1 ± 8.3	36.0 ± 0.8
	SAR [29]	57.5 ± 1.0	59.3 ± 0.2	49.6 ± 1.7	57.2 ± 1.1	43.7 ± 1.7	54.4 ± 1.5	59.4 ± 1.6	64.8 ± 1.0	65.4 ± 0.3	57.9 ± 0.4	77.1 ± 0.2	60.2 ± 1.8	50.0 ± 1.2	58.3 ± 0.6	59.8 ± 0.1	58.3 ± 0.3
	RoTTA [44]	64.4 ± 0.5	66.9 ± 0.8	56.1 ± 1.4	80.1 ± 0.4	59.1 ± 0.5	79.8 ± 0.2	82.2 ± 0.8	79.7 ± 0.8	78.7 ± 0.7	77.8 ± 0.4	91.2 ± 0.6	69.0 ± 4.0	72.3 ± 1.2	73.4 ± 0.2	72.8 ± 0.7	73.6 ± 0.5
	SoTTA	**73.3 ± 1.5**	**77.7 ± 0.8**	**66.8 ± 1.8**	**86.1 ± 2.1**	**64.0 ± 2.8**	**84.3 ± 0.7**	**86.6 ± 1.1**	**83.1 ± 0.7**	**82.0 ± 1.8**	**85.7 ± 2.7**	91.1 ± 0.4	**84.1 ± 2.4**	**77.1 ± 3.3**	**81.6 ± 2.8**	**77.2 ± 2.2**	**80.0 ± 1.4**

Table 6: Classification accuracy (%) and their corresponding standard deviations on CIFAR100-C for 15 types of corruptions under five scenarios. **Bold** numbers are the highest accuracy. Averaged over three different random seeds.

		Noise			Blur				Weather				Digital				
	Method	Gau.	Shot	Imp.	Def.	Gla.	Mot.	Zoom	Snow	Fro.	Fog	Brit.	Cont.	Elas.	Pix.	JPEG	Avg.
Benign	Source	10.6 ± 1.3	12.1 ± 1.2	7.2 ± 0.9	34.9 ± 0.3	19.6 ± 0.6	44.1 ± 0.6	41.9 ± 0.4	46.3 ± 0.2	34.2 ± 0.4	41.1 ± 0.9	67.3 ± 0.1	18.5 ± 0.6	50.4 ± 0.3	24.9 ± 2.5	44.6 ± 0.6	33.2 ± 0.4
	BN stats [27]	39.2 ± 0.9	40.7 ± 0.6	34.1 ± 0.7	66.1 ± 0.1	42.5 ± 0.4	63.6 ± 0.6	64.8 ± 0.1	53.8 ± 0.5	53.5 ± 0.2	58.1 ± 0.3	68.2 ± 0.2	64.5 ± 0.5	53.9 ± 0.4	56.6 ± 0.7	45.2 ± 0.3	53.7 ± 0.2
	PL [17]	46.5 ± 0.2	48.7 ± 0.9	40.8 ± 1.2	66.3 ± 0.5	45.5 ± 1.2	63.7 ± 0.7	65.7 ± 0.6	56.8 ± 0.6	55.1 ± 0.6	61.0 ± 0.2	68.6 ± 0.8	64.6 ± 0.6	54.6 ± 0.5	60.9 ± 0.4	49.6 ± 0.3	56.6 ± 0.2
	TENT [38]	50.0 ± 0.5	52.0 ± 0.8	44.2 ± 0.5	67.9 ± 0.3	48.7 ± 0.5	66.1 ± 0.5	68.0 ± 0.4	59.7 ± 0.5	59.3 ± 0.3	63.4 ± 0.2	70.8 ± 0.3	**67.3 ± 0.3**	57.5 ± 0.4	63.6 ± 0.3	53.7 ± 0.2	59.5 ± 0.0
	LAME [1]	7.8 ± 1.7	9.0 ± 1.7	5.9 ± 0.8	31.6 ± 0.3	16.6 ± 0.6	42.3 ± 0.8	39.8 ± 0.5	45.5 ± 0.2	31.7 ± 1.0	38.3 ± 1.1	66.4 ± 0.3	15.1 ± 0.6	49.5 ± 0.4	21.6 ± 2.8	43.9 ± 0.7	31.0 ± 0.5
	CoTTA [39]	47.5 ± 0.4	48.5 ± 0.5	43.2 ± 0.5	64.0 ± 0.3	46.4 ± 0.8	61.7 ± 0.8	62.8 ± 0.3	55.3 ± 0.8	56.1 ± 0.6	56.7 ± 0.4	68.1 ± 0.1	58.4 ± 0.7	54.3 ± 0.1	60.2 ± 0.4	53.4 ± 0.2	55.8 ± 0.4
	EATA [28]	11.1 ± 1.7	12.2 ± 1.3	7.2 ± 0.2	35.0 ± 1.2	10.4 ± 1.0	31.5 ± 4.6	39.6 ± 7.0	21.6 ± 1.8	17.9 ± 2.0	23.6 ± 3.2	56.4 ± 5.5	34.7 ± 5.6	15.2 ± 1.9	21.7 ± 3.4	14.7 ± 1.1	23.5 ± 1.9
	SAR [29]	46.5 ± 0.6	48.5 ± 0.8	40.9 ± 0.7	67.4 ± 0.3	46.1 ± 0.6	64.9 ± 0.8	66.3 ± 0.3	56.9 ± 0.5	56.4 ± 0.3	61.2 ± 0.4	69.8 ± 0.2	66.8 ± 0.5	56.1 ± 0.3	60.3 ± 0.4	50.8 ± 0.3	57.3 ± 0.3
	RoTTA [44]	35.7 ± 1.2	36.9 ± 1.1	31.6 ± 1.0	63.9 ± 0.3	40.3 ± 0.2	61.6 ± 0.7	63.0 ± 0.8	51.2 ± 0.5	44.1 ± 0.9	56.4 ± 0.2	66.1 ± 0.5	31.5 ± 1.4	52.3 ± 0.6	52.9 ± 1.1	43.1 ± 0.6	48.7 ± 0.6
	SoTTA	**52.0 ± 0.6**	**53.4 ± 0.4**	**45.0 ± 1.1**	**68.8 ± 0.2**	**49.1 ± 0.8**	**66.7 ± 0.6**	**69.0 ± 0.2**	**61.7 ± 0.6**	**60.2 ± 0.2**	**64.7 ± 0.6**	**72.2 ± 0.3**	66.4 ± 0.5	**58.6 ± 0.5**	**64.1 ± 0.2**	**55.0 ± 0.4**	**60.5 ± 0.0**
Near	Source	10.6 ± 1.3	12.1 ± 1.2	7.2 ± 0.9	34.9 ± 0.3	19.6 ± 0.6	44.1 ± 0.6	41.9 ± 0.4	46.3 ± 0.2	34.2 ± 0.4	41.1 ± 0.9	67.3 ± 0.1	18.5 ± 0.6	50.4 ± 0.3	24.9 ± 2.5	44.6 ± 0.6	33.2 ± 0.4
	BN stats [27]	36.0 ± 0.6	37.1 ± 0.6	31.5 ± 1.0	58.6 ± 0.3	37.7 ± 0.2	58.2 ± 0.1	60.1 ± 0.8	56.1 ± 0.4	56.1 ± 0.3	56.6 ± 0.1	71.7 ± 0.3	54.9 ± 0.5	52.4 ± 0.5	49.8 ± 0.7	45.4 ± 0.6	50.8 ± 0.1
	PL [17]	32.4 ± 2.0	32.1 ± 2.1	26.5 ± 1.7	58.4 ± 1.8	33.5 ± 0.6	56.9 ± 1.5	58.8 ± 1.9	51.5 ± 0.6	50.5 ± 1.5	53.4 ± 2.0	66.7 ± 1.2	51.4 ± 3.9	49.3 ± 0.9	53.1 ± 0.5	45.3 ± 0.8	48.0 ± 0.3
	TENT [38]	26.8 ± 5.6	27.1 ± 0.6	21.4 ± 2.9	58.7 ± 2.1	24.5 ± 2.1	58.0 ± 1.1	60.8 ± 0.8	50.6 ± 1.1	47.7 ± 2.2	52.6 ± 2.1	66.3 ± 1.2	58.2 ± 0.0	46.2 ± 0.3	52.1 ± 1.0	44.5 ± 1.6	46.4 ± 1.4
	LAME [1]	8.1 ± 1.6	9.6 ± 1.6	5.9 ± 0.9	32.6 ± 0.4	17.2 ± 0.5	43.0 ± 0.6	40.4 ± 0.6	45.7 ± 0.4	32.7 ± 0.7	39.1 ± 0.8	66.8 ± 0.1	15.6 ± 0.6	49.8 ± 0.4	22.3 ± 2.5	44.0 ± 0.6	31.5 ± 0.5
	CoTTA [39]	40.5 ± 0.8	41.3 ± 0.3	36.9 ± 0.5	51.5 ± 0.6	39.5 ± 0.5	53.4 ± 0.4	54.8 ± 0.9	56.8 ± 0.4	57.2 ± 0.5	52.6 ± 0.8	67.3 ± 0.1	38.2 ± 0.5	51.3 ± 0.9	56.4 ± 0.1	52.7 ± 0.3	50.0 ± 0.3
	EATA [28]	4.5 ± 0.9	4.3 ± 0.3	3.6 ± 0.3	7.4 ± 0.4	4.9 ± 0.3	7.6 ± 1.3	7.5 ± 0.6	7.0 ± 1.3	5.7 ± 1.0	5.8 ± 0.2	9.9 ± 1.3	5.2 ± 0.4	6.6 ± 0.3	5.7 ± 0.5	5.7 ± 0.7	6.1 ± 0.3
	SAR [29]	43.3 ± 0.1	44.6 ± 0.7	38.3 ± 0.9	62.6 ± 0.5	40.5 ± 0.3	61.5 ± 0.4	63.5 ± 0.8	58.6 ± 0.5	**58.5 ± 0.1**	61.4 ± 0.5	**72.1 ± 0.4**	62.0 ± 0.3	**54.6 ± 0.1**	57.5 ± 0.3	51.6 ± 0.5	55.4 ± 0.1
	RoTTA [44]	36.6 ± 0.7	38.6 ± 0.4	30.5 ± 1.5	64.0 ± 0.4	38.1 ± 0.1	61.9 ± 0.6	63.7 ± 0.5	55.1 ± 1.0	50.3 ± 2.2	58.4 ± 0.3	68.2 ± 0.6	26.6 ± 1.1	52.7 ± 0.6	52.3 ± 1.2	44.3 ± 1.0	49.4 ± 0.5
	SoTTA	**47.2 ± 1.1**	**48.5 ± 0.7**	**40.4 ± 1.8**	**64.8 ± 0.4**	**42.4 ± 0.3**	**63.4 ± 0.3**	**65.8 ± 0.5**	**59.1 ± 0.3**	58.2 ± 0.6	**62.2 ± 0.5**	70.8 ± 0.3	**65.8 ± 0.5**	54.3 ± 0.1	**60.7 ± 0.4**	**53.4 ± 0.7**	**57.1 ± 0.2**
Far	Source	10.6 ± 1.3	12.1 ± 1.2	7.2 ± 0.9	34.9 ± 0.3	19.6 ± 0.6	44.1 ± 0.6	41.9 ± 0.4	46.3 ± 0.2	34.2 ± 0.4	41.1 ± 0.9	67.3 ± 0.1	18.5 ± 0.6	50.4 ± 0.3	24.9 ± 2.5	44.6 ± 0.6	33.2 ± 0.4
	BN stats [27]	32.5 ± 0.4	34.4 ± 0.4	27.9 ± 0.7	59.1 ± 0.7	34.2 ± 0.3	56.3 ± 0.8	59.6 ± 0.2	48.4 ± 0.1	48.6 ± 0.2	53.5 ± 0.4	64.1 ± 0.4	51.9 ± 0.6	47.6 ± 0.7	46.9 ± 0.4	37.0 ± 0.4	46.8 ± 0.1
	PL [17]	24.7 ± 1.9	26.3 ± 3.6	19.7 ± 1.0	57.6 ± 1.1	26.1 ± 2.7	53.7 ± 1.7	57.5 ± 1.7	47.2 ± 1.8	44.0 ± 0.5	50.2 ± 1.4	62.1 ± 0.8	48.1 ± 1.8	42.0 ± 0.7	45.6 ± 2.1	37.0 ± 1.3	42.8 ± 0.7
	TENT [38]	17.3 ± 2.1	16.9 ± 2.0	13.9 ± 1.6	57.5 ± 2.2	19.8 ± 2.1	55.0 ± 0.5	60.0 ± 0.6	39.9 ± 5.2	40.8 ± 2.9	49.8 ± 2.7	63.6 ± 0.4	51.6 ± 4.5	37.0 ± 2.7	44.5 ± 3.7	32.7 ± 3.6	40.0 ± 1.3
	LAME [1]	7.8 ± 1.7	9.2 ± 1.8	5.9 ± 1.0	31.2 ± 0.9	17.0 ± 0.6	41.4 ± 1.2	38.5 ± 1.2	44.9 ± 0.4	31.9 ± 0.8	38.6 ± 1.1	65.5 ± 0.7	14.9 ± 0.9	49.2 ± 0.3	22.1 ± 2.6	43.3 ± 0.4	30.8 ± 0.7
	CoTTA [39]	32.1 ± 0.7	34.5 ± 1.2	28.6 ± 0.4	47.2 ± 0.9	32.7 ± 1.2	49.8 ± 0.4	51.1 ± 0.5	45.9 ± 2.5	46.7 ± 0.2	49.3 ± 0.7	56.7 ± 0.8	29.8 ± 0.7	44.0 ± 0.2	46.4 ± 0.8	41.8 ± 0.6	42.4 ± 0.4
	EATA [28]	3.3 ± 0.4	3.4 ± 0.5	3.2 ± 0.6	6.7 ± 0.9	3.6 ± 1.1	5.9 ± 0.5	6.8 ± 1.2	4.4 ± 0.7	4.5 ± 0.1	4.6 ± 1.0	7.2 ± 0.7	4.3 ± 1.0	4.1 ± 0.3	5.0 ± 0.8	4.8 ± 0.8	4.8 ± 0.5
	SAR [29]	37.4 ± 0.4	38.9 ± 1.1	32.2 ± 0.8	62.3 ± 0.3	36.9 ± 0.3	60.3 ± 0.1	63.3 ± 0.4	51.8 ± 0.3	52.5 ± 0.1	56.7 ± 0.7	66.8 ± 0.4	61.1 ± 1.0	50.4 ± 0.4	53.6 ± 0.7	44.2 ± 0.8	51.2 ± 0.1
	RoTTA [44]	39.3 ± 2.4	40.6 ± 2.2	35.2 ± 2.2	64.7 ± 0.3	42.3 ± 1.6	62.4 ± 0.6	63.7 ± 0.5	51.8 ± 0.9	45.3 ± 1.7	57.4 ± 0.3	66.2 ± 0.9	26.3 ± 0.7	52.6 ± 0.6	55.2 ± 1.1	44.0 ± 1.4	49.8 ± 0.9
	SoTTA	**50.8 ± 1.1**	**51.5 ± 0.9**	**42.3 ± 0.9**	**66.9 ± 0.5**	**46.2 ± 1.0**	**64.5 ± 0.3**	**67.3 ± 0.3**	**60.3 ± 0.0**	**59.5 ± 0.5**	**63.8 ± 0.1**	**70.7 ± 0.6**	**68.6 ± 0.9**	**55.8 ± 0.4**	**62.5 ± 0.4**	**54.0 ± 1.1**	**59.0 ± 0.4**
Attack	Source	10.6 ± 1.3	12.1 ± 1.2	7.2 ± 0.9	34.9 ± 0.3	19.6 ± 0.6	44.1 ± 0.6	41.9 ± 0.4	46.3 ± 0.2	34.2 ± 0.4	41.1 ± 0.9	67.3 ± 0.1	18.5 ± 0.6	50.4 ± 0.3	24.9 ± 2.5	44.6 ± 0.6	33.2 ± 0.4
	BN stats [27]	19.0 ± 0.4	19.5 ± 0.4	15.6 ± 0.7	36.2 ± 0.8	20.3 ± 0.3	37.7 ± 0.4	36.2 ± 0.6	31.2 ± 0.2	30.1 ± 0.4	31.2 ± 0.6	45.8 ± 0.4	35.2 ± 0.1	28.0 ± 0.4	30.8 ± 0.7	21.8 ± 0.5	29.2 ± 0.4
	PL [17]	33.8 ± 1.3	34.8 ± 0.8	29.0 ± 0.5	43.8 ± 1.3	29.3 ± 0.4	44.4 ± 0.2	45.1 ± 0.7	41.9 ± 0.1	40.1 ± 0.4	39.8 ± 0.2	53.7 ± 0.4	39.8 ± 0.3	36.0 ± 0.7	42.5 ± 0.2	35.3 ± 0.6	39.3 ± 0.4
	TENT [38]	28.7 ± 0.9	29.9 ± 1.0	23.3 ± 0.4	37.0 ± 1.0	21.7 ± 0.7	36.5 ± 0.6	37.4 ± 0.7	34.4 ± 0.4	32.6 ± 0.8	30.7 ± 0.7	46.4 ± 0.4	29.1 ± 1.5	26.5 ± 0.6	35.1 ± 0.4	29.0 ± 1.1	31.9 ± 0.7
	LAME [1]	7.6 ± 1.6	9.1 ± 1.6	5.9 ± 0.8	31.8 ± 0.5	16.4 ± 0.6	42.3 ± 0.7	39.4 ± 0.5	45.5 ± 0.3	31.9 ± 0.9	38.4 ± 1.1	66.3 ± 0.3	15.0 ± 0.7	49.4 ± 0.4	21.5 ± 2.7	43.7 ± 0.6	31.0 ± 0.6
	CoTTA [39]	34.4 ± 0.8	34.5 ± 0.6	29.9 ± 0.6	41.7 ± 1.0	31.1 ± 0.9	40.9 ± 0.4	42.5 ± 1.0	38.4 ± 0.2	37.8 ± 0.7	32.5 ± 0.4	50.6 ± 0.4	25.2 ± 0.8	35.3 ± 1.1	43.4 ± 0.3	39.8 ± 0.4	37.2 ± 0.2
	EATA [28]	2.2 ± 0.9	2.0 ± 0.7	2.5 ± 0.5	4.4 ± 0.1	1.7 ± 0.4	3.7 ± 0.8	3.8 ± 0.4	3.1 ± 0.3	2.8 ± 1.1	3.5 ± 0.6	15.1 ± 7.3	2.9 ± 0.7	2.5 ± 0.6	3.4 ± 0.7	2.7 ± 0.3	3.7 ± 0.6
	SAR [29]	27.0 ± 0.5	28.2 ± 0.6	23.1 ± 0.3	40.7 ± 0.6	24.3 ± 0.0	40.8 ± 0.1	40.6 ± 0.5	35.9 ± 0.2	34.7 ± 0.3	35.6 ± 0.4	49.3 ± 0.2	39.4 ± 0.1	31.0 ± 0.3	37.1 ± 0.6	28.5 ± 0.6	34.4 ± 0.3
	RoTTA [44]	40.5 ± 0.9	41.7 ± 0.7	35.9 ± 0.9	66.2 ± 0.3	43.5 ± 0.1	64.1 ± 0.7	65.5 ± 0.4	54.5 ± 0.3	49.5 ± 1.3	59.8 ± 0.0	68.3 ± 0.5	25.7 ± 4.0	54.7 ± 0.1	56.6 ± 0.6	46.2 ± 0.7	51.5 ± 0.4
	SoTTA	**54.3 ± 0.7**	**55.6 ± 0.7**	**47.6 ± 0.2**	**69.6 ± 0.2**	**51.6 ± 0.5**	**67.8 ± 0.1**	**69.7 ± 0.2**	**62.7 ± 0.3**	**61.7 ± 0.3**	**66.2 ± 0.1**	**72.5 ± 0.1**	**68.3 ± 1.2**	**59.4 ± 0.5**	**65.3 ± 0.4**	**56.5 ± 0.6**	**61.9 ± 0.0**
Noise	Source	10.6 ± 1.3	12.1 ± 1.2	7.2 ± 0.9	34.9 ± 0.3	19.6 ± 0.6	44.1 ± 0.6	41.9 ± 0.4	46.3 ± 0.2	34.2 ± 0.4	41.1 ± 0.9	67.3 ± 0.1	18.5 ± 0.6	50.4 ± 0.3	24.9 ± 2.5	44.6 ± 0.6	33.2 ± 0.4
	BN stats [27]	25.5 ± 1.0	25.5 ± 0.5	20.8 ± 0.9	28.2 ± 0.5	22.0 ± 0.1	28.4 ± 0.3	31.0 ± 0.4	30.7 ± 0.6	32.6 ± 0.3	24.5 ± 0.2	44.2 ± 0.5	25.8 ± 0.5	26.3 ± 0.2	29.4 ± 0.8	29.4 ± 0.6	28.3 ± 0.3
	PL [17]	21.4 ± 2.4	25.6 ± 3.4	15.8 ± 2.4	22.5 ± 2.1	16.1 ± 0.2	19.8 ± 2.3	23.8 ± 1.0	28.1 ± 0.3	30.7 ± 0.5	21.1 ± 1.4	47.4 ± 1.6	14.0 ± 2.1	21.6 ± 2.6	26.4 ± 4.5	23.4 ± 2.6	23.8 ± 0.6
	TENT [38]	16.4 ± 3.0	17.3 ± 5.5	11.3 ± 3.3	20.1 ± 4.2	11.2 ± 0.1	17.8 ± 2.3	24.3 ± 1.9	20.0 ± 2.7	24.6 ± 4.6	16.3 ± 1.5	50.9 ± 1.8	10.9 ± 1.6	13.5 ± 0.8	25.3 ± 3.8	19.5 ± 1.8	20.0 ± 0.9
	LAME [1]	7.9 ± 1.6	9.2 ± 1.7	6.1 ± 0.8	32.0 ± 0.5	16.5 ± 0.6	42.5 ± 1.0	39.8 ± 0.7	45.0 ± 1.0	31.9 ± 1.2	38.8 ± 1.1	66.2 ± 0.5	15.1 ± 0.9	49.8 ± 0.4	21.7 ± 2.7	43.6 ± 0.2	31.1 ± 0.7
	CoTTA [39]	28.6 ± 0.9	28.4 ± 0.3	25.3 ± 0.7	25.6 ± 0.8	21.8 ± 1.1	25.3 ± 1.5	28.2 ± 0.7	28.4 ± 1.4	31.0 ± 0.4	20.4 ± 0.4	38.2 ± 1.2	20.1 ± 0.5	25.1 ± 0.9	33.3 ± 0.7	30.4 ± 0.8	27.3 ± 0.3
	EATA [28]	2.8 ± 1.5	2.7 ± 0.6	2.3 ± 0.3	2.6 ± 0.3	2.0 ± 0.6	2.0 ± 0.3	2.8 ± 0.3	1.9 ± 0.1	2.4 ± 0.4	2.0 ± 0.2	2.7 ± 0.7	2.2 ± 0.3	3.0 ± 0.3	2.1 ± 0.3	2.6 ± 0.2	2.4 ± 0.2
	SAR [29]	37.5 ± 1.9	37.8 ± 2.1	29.3 ± 2.9	38.8 ± 0.5	26.4 ± 2.4	38.9 ± 2.2	42.4 ± 1.0	41.2 ± 3.9	42.7 ± 0.5	36.4 ± 2.5	57.2 ± 0.8	32.1 ± 1.3	32.9 ± 3.5	40.7 ± 1.8	37.7 ± 1.2	38.1 ± 1.2
	RoTTA [44]	36.6 ± 1.0	37.9 ± 1.5	31.2 ± 1.4	61.9 ± 1.0	40.4 ± 0.4	60.7 ± 0.3	61.9 ± 0.6	51.7 ± 0.5	45.7 ± 0.7	55.9 ± 0.4	66.5 ± 0.4	25.5 ± 1.5	51.6 ± 0.7	53.0 ± 0.9	44.5 ± 1.0	48.3 ± 0.5
	SoTTA	**50.4 ± 2.5**	**52.3 ± 0.7**	**41.9 ± 3.5**	**66.3 ± 0.8**	**45.5 ± 0.7**	**65.4 ± 0.5**	**66.7 ± 0.6**	**60.1 ± 0.9**	**59.3 ± 0.2**	**63.1 ± 1.0**	**70.7 ± 0.3**	**65.6 ± 1.1**	**55.9 ± 1.4**	**61.8 ± 1.9**	**54.6 ± 0.6**	**58.6 ± 1.0**

Table 7: Classification accuracy (%) and their corresponding standard deviations on ImageNet-C for 15 types of corruptions under five scenarios. **Bold** numbers are the highest accuracy. Averaged over three different random seeds.

		Noise			Blur				Weather				Digital				
	Method	Gau.	Shot	Imp.	Def.	Gla.	Mot.	Zoom	Snow	Fro.	Fog	Brit.	Cont.	Elas.	Pix.	JPEG	Avg.
Benign	Source	1.2 ±0.0	1.8 ±0.0	1.0 ±0.0	11.4 ±0.0	8.7 ±0.0	11.2 ±0.0	17.6 ±0.0	10.9 ±0.0	16.5 ±0.0	14.3 ±0.0	51.3 ±0.0	3.4 ±0.0	16.8 ±0.0	23.1 ±0.0	29.6 ±0.0	14.6 ±0.0
	BN stats [27]	13.0 ±0.1	14.1 ±0.1	13.4 ±0.0	11.7 ±0.0	12.8 ±0.0	23.1 ±0.1	33.3 ±0.0	29.1 ±0.1	28.1 ±0.0	40.3 ±0.1	57.7 ±0.1	11.9 ±0.1	38.4 ±0.0	43.8 ±0.1	36.4 ±0.1	27.1 ±0.0
	PL [17]	14.9 ±1.2	18.3 ±1.3	16.5 ±0.7	11.2 ±0.7	13.2 ±1.2	29.1 ±1.6	39.1 ±0.5	35.5 ±1.1	26.0 ±1.2	47.6 ±0.6	58.3 ±0.3	5.2 ±0.3	46.5 ±0.6	50.5 ±0.2	45.6 ±0.1	30.5 ±0.1
	TENT [38]	13.0 ±0.1	14.1 ±0.1	13.4 ±0.0	11.7 ±0.0	12.8 ±0.0	23.1 ±0.1	33.3 ±0.0	29.1 ±0.1	28.1 ±0.0	40.3 ±0.1	57.7 ±0.1	11.9 ±0.1	38.4 ±0.0	43.8 ±0.1	36.4 ±0.1	27.1 ±0.0
	LAME [1]	0.7 ±0.0	1.1 ±0.0	0.5 ±0.0	11.4 ±0.0	8.6 ±0.0	11.1 ±0.0	17.5 ±0.0	10.3 ±0.0	16.4 ±0.0	14.1 ±0.0	51.3 ±0.0	3.4 ±0.0	16.5 ±0.0	23.0 ±0.0	29.6 ±0.0	14.4 ±0.0
	CoTTA [39]	17.7 ±0.1	19.0 ±0.2	18.0 ±0.1	15.7 ±0.1	17.4 ±0.3	30.6 ±0.1	39.0 ±0.2	34.0 ±0.3	32.4 ±0.1	46.9 ±0.2	59.3 ±0.1	18.7 ±0.3	43.1 ±0.1	49.8 ±0.2	42.2 ±0.1	32.2 ±0.1
	EATA [28]	25.9 ±0.2	27.5 ±0.1	25.9 ±0.2	23.7 ±0.4	23.9 ±0.4	35.2 ±0.3	43.2 ±0.0	40.2 ±0.2	36.2 ±0.2	50.3 ±0.1	59.9 ±0.0	**30.6 ±0.3**	48.4 ±0.0	51.8 ±0.0	47.0 ±0.1	38.0 ±0.1
	SAR [29]	24.5 ±0.3	26.4 ±0.1	24.5 ±0.2	21.0 ±0.1	21.6 ±0.2	33.3 ±0.0	41.1 ±0.1	38.3 ±0.1	34.6 ±0.1	49.2 ±0.1	59.4 ±0.1	24.8 ±1.0	46.5 ±0.1	50.7 ±0.2	45.8 ±0.0	36.1 ±0.1
	RoTTA [44]	15.1 ±0.1	16.5 ±0.2	15.5 ±0.1	13.1 ±0.2	14.2 ±0.0	25.5 ±0.1	36.1 ±0.1	31.8 ±0.2	28.9 ±0.1	44.2 ±0.2	59.5 ±0.0	15.6 ±0.2	41.6 ±0.1	46.8 ±0.0	40.3 ±0.1	29.7 ±0.0
	SoTTA	**29.2 ±0.2**	**31.8 ±0.3**	**29.8 ±0.3**	**26.2 ±0.2**	**27.6 ±0.2**	**37.9 ±0.2**	**44.7 ±0.2**	**42.8 ±0.2**	**37.9 ±0.3**	**52.3 ±0.2**	**60.1 ±0.1**	24.1 ±0.5	**50.3 ±0.1**	**53.4 ±0.1**	**48.7 ±0.2**	**39.8 ±0.0**
Near	Source	1.2 ±0.0	1.8 ±0.0	1.0 ±0.0	11.4 ±0.0	8.7 ±0.0	11.2 ±0.0	17.6 ±0.0	10.9 ±0.0	16.5 ±0.0	14.3 ±0.0	51.3 ±0.0	3.4 ±0.0	16.8 ±0.0	23.1 ±0.0	29.6 ±0.0	14.6 ±0.0
	BN stats [27]	5.8 ±0.5	6.9 ±0.1	6.7 ±0.0	8.5 ±0.7	8.5 ±0.3	15.5 ±0.0	24.6 ±0.1	19.1 ±0.4	21.5 ±0.1	26.8 ±0.0	49.7 ±0.1	4.5 ±0.2	26.2 ±0.1	31.7 ±0.0	27.3 ±0.2	18.9 ±0.1
	PL [17]	0.5 ±0.1	0.7 ±0.1	0.6 ±0.0	2.2 ±0.1	1.6 ±0.3	4.4 ±0.2	7.2 ±0.5	3.8 ±0.4	3.6 ±0.2	11.4 ±0.8	35.6 ±1.3	0.6 ±0.0	6.5 ±1.3	18.7 ±0.6	5.7 ±0.2	6.9 ±0.0
	TENT [38]	5.8 ±0.5	6.9 ±0.1	6.7 ±0.0	8.5 ±0.7	8.5 ±0.3	15.5 ±0.0	24.6 ±0.1	19.1 ±0.4	21.5 ±0.1	26.8 ±0.0	49.7 ±0.1	4.5 ±0.2	26.2 ±0.1	31.7 ±0.0	27.3 ±0.2	18.9 ±0.1
	LAME [1]	1.0 ±0.1	1.5 ±0.0	0.8 ±0.0	10.8 ±1.0	8.4 ±0.3	11.1 ±0.0	17.5 ±0.0	10.3 ±0.2	16.4 ±0.0	14.1 ±0.0	51.3 ±0.0	3.4 ±0.1	16.5 ±0.0	23.0 ±0.0	29.6 ±0.0	14.4 ±0.1
	CoTTA [39]	6.6 ±0.9	7.8 ±0.2	7.4 ±0.1	11.6 ±1.7	11.1 ±0.2	23.1 ±0.1	30.5 ±0.2	24.6 ±0.4	24.8 ±0.0	36.0 ±0.1	53.7 ±0.3	5.8 ±1.1	31.8 ±0.1	41.4 ±0.1	34.0 ±0.3	23.3 ±0.2
	EATA [28]	6.6 ±0.1	9.1 ±0.1	7.7 ±0.2	14.1 ±0.0	12.9 ±0.1	23.3 ±0.2	33.5 ±0.1	29.0 ±0.0	28.9 ±0.2	40.1 ±0.1	55.4 ±0.1	**6.4 ±0.8**	36.9 ±0.3	43.7 ±0.3	36.5 ±0.1	25.6 ±0.1
	SAR [29]	**6.7 ±1.3**	**10.2 ±0.6**	**8.1 ±0.6**	15.9 ±1.9	13.5 ±0.7	**28.1 ±0.1**	37.0 ±0.1	32.9 ±1.3	28.2 ±0.5	44.6 ±0.2	56.8 ±0.0	1.8 ±0.5	40.8 ±0.4	47.7 ±0.1	41.6 ±0.3	27.6 ±0.3
	RoTTA [44]	3.1 ±0.7	5.4 ±1.0	3.7 ±0.4	10.8 ±1.0	9.2 ±0.6	23.0 ±0.4	33.5 ±1.3	32.3 ±0.8	**30.3 ±0.2**	44.6 ±0.0	**59.3 ±0.1**	0.7 ±0.1	40.2 ±0.0	46.3 ±0.3	40.2 ±0.2	25.6 ±0.4
	SoTTA	0.3 ±0.1	5.8 ±4.0	0.5 ±0.2	**21.7 ±0.8**	**21.5 ±0.8**	26.9 ±4.9	**39.0 ±0.6**	**35.0 ±0.5**	28.1 ±0.5	**46.5 ±0.2**	56.1 ±0.2	0.5 ±0.1	**44.8 ±0.1**	**49.2 ±0.3**	**43.2 ±0.1**	**27.9 ±0.3**
Far	Source	1.2 ±0.0	1.8 ±0.0	1.0 ±0.0	11.4 ±0.0	8.7 ±0.0	11.2 ±0.0	17.6 ±0.0	10.9 ±0.0	16.5 ±0.0	14.3 ±0.0	51.3 ±0.0	3.4 ±0.0	16.8 ±0.0	23.1 ±0.0	29.6 ±0.0	14.6 ±0.0
	BN stats [27]	4.5 ±0.0	5.0 ±0.1	5.0 ±0.0	4.2 ±0.0	5.3 ±0.0	9.1 ±0.1	16.2 ±0.1	17.4 ±0.1	18.0 ±0.0	22.2 ±0.1	43.3 ±0.1	1.2 ±0.0	23.2 ±0.1	26.9 ±0.0	20.9 ±0.1	14.8 ±0.0
	PL [17]	0.4 ±0.0	0.5 ±0.0	0.5 ±0.1	0.7 ±0.2	1.0 ±0.2	1.4 ±0.1	3.4 ±0.4	2.2 ±0.2	2.8 ±0.1	6.6 ±2.1	34.7 ±5.1	0.2 ±0.0	6.3 ±0.5	12.2 ±1.4	4.3 ±0.3	5.1 ±0.2
	TENT [38]	4.5 ±0.0	5.0 ±0.1	5.0 ±0.0	4.2 ±0.0	5.3 ±0.0	9.2 ±0.1	16.2 ±0.1	17.4 ±0.1	18.0 ±0.0	22.2 ±0.1	43.3 ±0.1	1.2 ±0.0	23.2 ±0.1	26.9 ±0.0	20.9 ±0.1	14.8 ±0.0
	LAME [1]	0.7 ±0.0	1.1 ±0.0	0.5 ±0.0	11.4 ±0.0	8.6 ±0.0	11.1 ±0.0	17.5 ±0.0	10.3 ±0.0	16.3 ±0.0	14.0 ±0.0	51.3 ±0.0	3.3 ±0.0	16.5 ±0.0	23.0 ±0.0	29.6 ±0.0	14.4 ±0.0
	CoTTA [39]	4.4 ±0.5	5.1 ±0.7	4.5 ±0.2	4.2 ±0.3	6.2 ±0.2	10.7 ±0.8	18.9 ±0.7	21.6 ±1.0	20.0 ±0.8	30.0 ±0.2	48.2 ±0.3	0.9 ±0.4	27.9 ±0.9	34.8 ±0.7	27.0 ±0.2	17.6 ±0.2
	EATA [28]	7.9 ±0.6	10.1 ±0.5	10.1 ±0.4	8.9 ±0.5	10.2 ±0.2	17.9 ±0.4	28.8 ±0.3	27.1 ±0.3	26.8 ±0.2	38.2 ±0.1	52.2 ±0.2	0.8 ±0.1	34.3 ±0.2	40.2 ±0.2	32.6 ±0.1	23.1 ±0.1
	SAR [29]	3.2 ±0.5	4.9 ±1.2	3.7 ±1.2	3.5 ±1.7	5.5 ±1.7	20.6 ±1.5	32.1 ±0.9	31.8 ±0.2	26.1 ±0.9	43.1 ±0.1	54.0 ±0.2	0.4 ±0.1	39.2 ±0.5	45.4 ±0.2	39.1 ±0.1	23.5 ±0.4
	RoTTA [44]	13.9 ±0.1	15.5 ±0.1	16.2 ±0.1	12.1 ±0.1	12.8 ±0.1	25.0 ±0.1	35.8 ±0.2	33.6 ±0.2	29.5 ±1.9	45.8 ±0.8	**59.4 ±0.2**	**8.0 ±0.2**	41.9 ±0.1	47.0 ±0.1	41.0 ±0.3	29.2 ±0.2
	SoTTA	**26.9 ±0.4**	**29.5 ±0.4**	**27.3 ±0.1**	**22.3 ±0.2**	**23.6 ±0.6**	**35.8 ±0.4**	**42.2 ±0.1**	**40.8 ±0.6**	**35.5 ±0.1**	**50.7 ±0.4**	58.4 ±0.7	1.6 ±1.1	**48.3 ±0.3**	**52.2 ±0.3**	**46.8 ±0.2**	**36.1 ±0.1**
Attack	Source	1.2 ±0.0	1.8 ±0.0	1.0 ±0.0	11.4 ±0.0	8.7 ±0.0	11.2 ±0.0	17.6 ±0.0	10.9 ±0.0	16.5 ±0.0	14.3 ±0.0	51.3 ±0.0	3.4 ±0.0	16.8 ±0.0	23.1 ±0.0	29.6 ±0.0	14.6 ±0.0
	BN stats [27]	6.4 ±0.0	7.7 ±0.1	6.7 ±0.0	7.2 ±0.1	7.3 ±0.1	12.5 ±0.9	20.0 ±0.1	19.2 ±0.2	17.6 ±0.1	24.8 ±0.1	46.1 ±0.1	10.5 ±0.1	25.1 ±0.1	24.5 ±10.3	24.9 ±0.1	17.4 ±0.8
	PL [17]	6.5 ±0.7	7.8 ±0.5	6.3 ±0.4	4.0 ±0.2	4.4 ±0.3	10.5 ±0.6	22.2 ±2.7	20.0 ±1.7	9.7 ±0.7	28.8 ±0.4	48.6 ±0.4	1.9 ±0.2	34.5 ±2.8	29.8 ±18.9	36.0 ±0.6	18.1 ±1.3
	TENT [38]	6.4 ±0.0	7.7 ±0.1	6.7 ±0.0	7.2 ±0.1	7.3 ±0.1	12.5 ±0.9	20.0 ±0.1	19.2 ±0.2	17.6 ±0.1	24.8 ±0.1	46.1 ±0.1	10.5 ±0.1	25.1 ±0.1	24.5 ±10.3	25.0 ±0.1	17.4 ±0.8
	LAME [1]	0.7 ±0.0	1.1 ±0.0	0.5 ±0.0	11.4 ±0.0	8.6 ±0.0	10.7 ±0.6	17.5 ±0.0	10.3 ±0.0	16.4 ±0.0	14.1 ±0.0	51.3 ±0.0	3.4 ±0.0	16.5 ±0.0	18.5 ±7.7	29.6 ±0.0	14.0 ±0.6
	CoTTA [39]	17.2 ±0.2	18.6 ±0.2	17.3 ±0.2	14.5 ±0.1	15.0 ±0.1	27.0 ±2.4	32.7 ±0.1	31.9 ±0.2	28.3 ±0.2	40.2 ±0.2	52.0 ±0.1	18.8 ±0.3	38.6 ±0.2	34.3 ±16.2	38.7 ±0.1	28.3 ±1.3
	EATA [28]	15.3 ±0.1	17.5 ±0.2	15.5 ±0.2	13.9 ±0.2	12.9 ±0.2	22.0 ±0.1	28.8 ±0.2	29.0 ±0.4	24.3 ±0.1	35.5 ±0.1	49.2 ±0.1	17.3 ±0.8	35.7 ±0.2	39.1 ±0.1	36.0 ±0.1	26.1 ±0.1
	SAR [29]	19.1 ±0.1	21.2 ±0.0	18.8 ±0.1	15.6 ±0.2	15.1 ±0.2	22.5 ±2.1	29.1 ±0.1	29.5 ±0.3	25.2 ±0.0	35.8 ±0.1	49.0 ±0.1	17.3 ±1.2	35.8 ±0.1	31.4 ±14.0	36.7 ±0.0	26.8 ±1.0
	RoTTA [44]	19.0 ±0.2	19.7 ±0.3	19.1 ±0.1	16.8 ±0.1	17.1 ±0.2	28.9 ±1.8	38.4 ±0.1	35.7 ±0.2	31.1 ±0.2	47.0 ±0.1	59.8 ±0.1	22.0 ±0.0	43.5 ±0.1	39.1 ±16.7	43.3 ±0.1	32.0 ±1.2
	SoTTA	**30.9 ±0.3**	**33.5 ±0.2**	**31.7 ±0.2**	**28.3 ±0.3**	**29.4 ±0.0**	**40.0 ±0.3**	**45.4 ±0.2**	**44.2 ±0.2**	**38.9 ±0.2**	**53.1 ±0.1**	**60.5 ±0.0**	**25.4 ±1.4**	**54.5 ±0.2**	**49.5 ±0.2**	**41.1 ±0.1**	**41.1 ±0.1**
Noise	Source	1.2 ±0.0	1.8 ±0.0	1.0 ±0.0	11.4 ±0.0	8.7 ±0.0	11.2 ±0.0	17.6 ±0.0	10.9 ±0.0	16.5 ±0.0	14.3 ±0.0	51.3 ±0.0	3.4 ±0.0	16.8 ±0.0	23.1 ±0.0	29.6 ±0.0	14.6 ±0.0
	BN stats [27]	7.0 ±0.1	7.5 ±0.1	7.4 ±0.0	5.1 ±0.1	6.0 ±0.0	7.5 ±0.0	11.9 ±0.1	12.4 ±0.1	11.4 ±0.0	10.7 ±0.1	34.5 ±0.1	4.4 ±0.1	16.3 ±0.1	23.9 ±0.1	25.7 ±0.1	12.8 ±0.0
	PL [17]	0.5 ±0.1	0.9 ±0.4	1.1 ±0.3	0.6 ±0.1	0.6 ±0.1	0.7 ±0.1	1.5 ±0.2	1.6 ±0.2	1.4 ±0.1	1.1 ±0.4	19.0 ±5.7	0.5 ±0.1	2.8 ±1.4	11.2 ±2.6	7.7 ±1.9	3.4 ±0.6
	TENT [38]	7.0 ±0.1	7.5 ±0.1	7.4 ±0.0	5.1 ±0.1	6.0 ±0.0	7.6 ±0.1	11.8 ±0.1	12.3 ±0.1	11.3 ±0.0	10.6 ±0.1	34.5 ±0.1	4.5 ±0.1	16.3 ±0.1	23.9 ±0.1	25.6 ±0.1	12.8 ±0.0
	LAME [1]	0.7 ±0.0	1.1 ±0.0	0.5 ±0.0	11.4 ±0.0	8.5 ±0.0	11.1 ±0.0	17.5 ±0.0	10.3 ±0.0	16.4 ±0.0	14.0 ±0.0	51.3 ±0.0	3.4 ±0.0	16.5 ±0.0	23.0 ±0.0	29.6 ±0.0	14.3 ±0.0
	CoTTA [39]	8.3 ±0.1	9.0 ±0.8	9.2 ±0.0	4.3 ±0.4	5.4 ±0.3	7.8 ±0.2	13.3 ±0.8	16.6 ±0.1	13.7 ±0.0	14.9 ±0.7	44.0 ±0.8	3.2 ±0.6	19.4 ±0.1	30.9 ±1.2	32.3 ±0.4	16.0 ±0.9
	EATA [28]	14.0 ±0.1	14.8 ±0.2	14.3 ±0.4	8.5 ±0.3	9.0 ±0.4	12.4 ±0.3	21.1 ±0.4	22.0 ±0.5	19.5 ±0.2	24.6 ±0.3	46.6 ±0.2	2.1 ±0.4	28.0 ±0.3	37.3 ±0.3	36.5 ±0.2	20.7 ±0.2
	SAR [29]	13.9 ±4.0	18.8 ±1.5	16.3 ±0.5	5.1 ±1.2	3.4 ±0.3	6.6 ±2.1	25.0 ±0.4	27.6 ±0.5	19.8 ±1.7	33.9 ±0.2	49.8 ±0.1	1.0 ±0.1	29.0 ±1.4	41.2 ±0.1	38.3 ±1.4	22.0 ±0.4
	RoTTA [44]	16.2 ±0.2	17.2 ±0.4	16.5 ±0.2	17.7 ±0.1	16.6 ±0.1	26.8 ±0.0	37.3 ±0.1	33.4 ±0.2	29.3 ±0.4	45.0 ±0.1	**59.4 ±0.1**	21.0 ±0.3	42.4 ±0.1	48.2 ±0.2	41.3 ±1.5	31.2 ±0.2
	SoTTA	**27.5 ±0.6**	**30.4 ±0.2**	**28.3 ±0.1**	**26.5 ±0.3**	**27.3 ±0.4**	**37.7 ±0.1**	**43.6 ±0.1**	**42.4 ±0.2**	**36.9 ±0.6**	**51.6 ±0.1**	59.2 ±0.1	**23.8 ±0.3**	**49.6 ±0.3**	**53.0 ±0.1**	**48.2 ±0.1**	**39.0 ±0.1**

Table 8: Classification accuracy (%) and their corresponding standard deviations on ablation study of individual components on CIFAR10-C for 15 types of corruptions under five scenarios. **Bold** numbers are the highest accuracy. Averaged over three different random seeds.

		Noise			Blur				Weather				Digital				
	Method	Gau.	Shot	Imp.	Def.	Gla.	Mot.	Zoom	Snow	Fro.	Fog	Brit.	Cont.	Elas.	Pix.	JPEG	Avg.
Benign	Source	26.0 ± 3.3	33.2 ± 3.5	24.7 ± 4.2	56.7 ± 2.7	52.0 ± 2.7	67.4 ± 1.2	64.8 ± 2.6	78.0 ± 0.4	67.0 ± 2.5	74.1 ± 0.8	91.5 ± 0.3	33.9 ± 1.8	76.6 ± 0.7	46.4 ± 0.6	73.2 ± 0.8	57.7 ± 1.0
	HC	10.2 ± 0.1	10.9 ± 0.9	10.7 ± 0.7	61.9 ± 31.5	14.2 ± 0.4	41.8 ± 21.6	82.0 ± 2.0	32.1 ± 11.6	36.3 ± 17.7	52.3 ± 28.7	88.7 ± 1.1	11.2 ± 1.3	34.0 ± 15.8	14.2 ± 3.9	23.5 ± 3.8	34.9 ± 4.8
	UC	26.0 ± 19.5	42.0 ± 27.4	10.5 ± 0.5	82.4 ± 0.8	59.0 ± 1.2	79.3 ± 1.8	82.5 ± 1.4	77.5 ± 1.2	76.5 ± 1.5	81.5 ± 0.6	86.3 ± 1.5	73.2 ± 6.0	73.3 ± 1.1	74.9 ± 1.6	71.4 ± 1.4	66.4 ± 3.0
	HC + UC (HUS)	20.7 ± 15.1	57.8 ± 4.7	21.1 ± 9.5	84.6 ± 0.9	62.4 ± 1.8	83.4 ± 0.5	85.2 ± 1.1	80.5 ± 1.4	79.3 ± 0.5	84.5 ± 1.0	89.8 ± 0.3	69.5 ± 11.5	76.4 ± 1.3	76.3 ± 2.2	75.1 ± 0.4	69.8 ± 1.1
	ESM	**76.0 ± 0.6**	**78.3 ± 0.4**	**69.3 ± 0.5**	**89.0 ± 0.2**	69.7 ± 1.7	**87.9 ± 0.4**	**89.6 ± 0.2**	85.3 ± 0.4	84.1 ± 0.7	87.7 ± 0.3	92.1 ± 0.2	**88.1 ± 0.8**	79.6 ± 1.0	84.2 ± 0.4	**78.5 ± 0.3**	**82.6 ± 0.2**
	HC + ESM	74.9 ± 0.8	78.1 ± 0.0	69.0 ± 0.6	88.8 ± 0.3	70.9 ± 0.6	87.7 ± 0.6	89.2 ± 0.1	**85.7 ± 0.5**	**84.4 ± 0.1**	87.8 ± 0.1	**92.2 ± 0.3**	84.0 ± 0.6	79.7 ± 0.7	83.7 ± 0.8	78.1 ± 0.4	82.3 ± 0.2
	UC + ESM	74.9 ± 0.5	77.1 ± 1.1	68.2 ± 0.5	88.7 ± 0.4	**71.0 ± 1.5**	87.4 ± 0.3	89.1 ± 1.0	85.0 ± 0.5	84.0 ± 0.3	87.8 ± 0.9	92.0 ± 0.3	86.2 ± 2.4	**79.8 ± 1.0**	**84.4 ± 0.6**	78.0 ± 0.8	82.2 ± 0.2
	HUS + ESM (SoTTA)	75.0 ± 1.1	77.5 ± 0.6	68.8 ± 0.7	88.8 ± 0.4	70.7 ± 1.2	87.5 ± 0.5	89.0 ± 0.5	85.4 ± 0.3	84.0 ± 0.7	**88.2 ± 0.2**	91.9 ± 0.1	83.9 ± 1.5	**79.8 ± 0.4**	83.9 ± 0.5	78.3 ± 0.7	82.2 ± 0.3
Near	Source	26.0 ± 3.3	33.2 ± 3.5	24.7 ± 4.2	56.7 ± 2.7	52.0 ± 2.7	67.4 ± 1.2	64.8 ± 2.6	78.0 ± 0.4	67.0 ± 2.5	74.1 ± 0.8	**91.5 ± 0.3**	33.9 ± 1.8	76.6 ± 0.7	46.4 ± 0.6	73.2 ± 0.8	57.7 ± 1.0
	HC	10.3 ± 0.1	10.6 ± 0.3	10.1 ± 0.0	12.6 ± 2.9	12.3 ± 2.5	11.9 ± 0.5	16.7 ± 4.8	16.1 ± 1.9	14.4 ± 1.4	14.5 ± 2.4	16.6 ± 0.6	11.2 ± 1.5	19.7 ± 3.6	13.2 ± 1.2	14.0 ± 0.7	13.6 ± 0.3
	UC	42.6 ± 6.6	48.3 ± 2.4	20.8 ± 4.5	73.3 ± 2.2	50.4 ± 3.9	73.1 ± 1.8	74.9 ± 3.3	71.0 ± 2.2	67.5 ± 1.9	74.7 ± 4.7	82.4 ± 0.9	59.7 ± 1.9	64.3 ± 0.8	64.9 ± 5.6	64.2 ± 1.9	62.1 ± 0.8
	HC + UC (HUS)	32.8 ± 2.5	42.5 ± 3.5	15.9 ± 7.3	73.8 ± 2.5	51.1 ± 2.1	73.8 ± 1.9	77.8 ± 2.8	65.1 ± 13.4	70.8 ± 1.1	77.6 ± 0.5	84.6 ± 0.8	61.6 ± 2.7	69.7 ± 1.2	62.6 ± 4.7	66.2 ± 3.2	61.7 ± 1.3
	ESM	67.9 ± 1.4	69.7 ± 0.5	58.5 ± 0.6	84.6 ± 1.4	63.0 ± 3.5	83.9 ± 0.8	86.7 ± 0.1	82.5 ± 0.4	81.3 ± 0.5	85.2 ± 0.6	90.6 ± 0.4	83.3 ± 2.5	77.9 ± 1.9	76.7 ± 1.5	76.0 ± 1.5	77.9 ± 0.4
	HC + ESM	73.6 ± 1.4	75.6 ± 1.7	64.3 ± 3.9	87.3 ± 1.0	66.7 ± 0.6	86.3 ± 0.7	87.6 ± 0.5	**84.8 ± 0.2**	83.2 ± 0.3	86.9 ± 0.9	90.9 ± 0.7	87.3 ± 0.5	**79.1 ± 0.9**	82.3 ± 0.8	77.3 ± 1.3	80.9 ± 0.6
	UC + ESM	68.1 ± 2.3	69.4 ± 0.9	60.3 ± 2.9	84.8 ± 0.6	64.6 ± 2.3	84.2 ± 1.1	85.5 ± 0.2	82.2 ± 0.6	81.7 ± 1.7	85.3 ± 0.7	90.8 ± 0.4	84.4 ± 1.0	77.0 ± 1.2	75.5 ± 0.1	76.5 ± 0.9	78.0 ± 0.4
	HUS + ESM (SoTTA)	**74.3 ± 1.4**	**76.7 ± 0.9**	**66.5 ± 2.2**	**87.5 ± 0.1**	**66.9 ± 0.8**	**86.4 ± 0.6**	**87.8 ± 0.5**	84.4 ± 0.6	**83.8 ± 0.2**	**87.2 ± 0.5**	91.3 ± 0.2	**88.4 ± 0.7**	78.7 ± 1.1	**82.4 ± 0.5**	**78.0 ± 0.6**	**81.4 ± 0.5**
Far	Source	26.0 ± 3.3	33.2 ± 3.5	24.7 ± 4.2	56.7 ± 2.7	52.0 ± 2.7	67.4 ± 1.2	64.8 ± 2.6	78.0 ± 0.4	67.0 ± 2.5	74.1 ± 0.8	91.5 ± 0.3	33.9 ± 1.8	76.6 ± 0.7	46.4 ± 0.6	73.2 ± 0.8	57.7 ± 1.0
	HC	10.3 ± 0.1	10.7 ± 0.8	10.1 ± 0.0	15.4 ± 7.3	12.1 ± 0.7	17.4 ± 6.7	26.7 ± 22.2	16.2 ± 3.1	16.6 ± 2.6	17.9 ± 7.7	55.5 ± 28.4	11.0 ± 0.7	15.3 ± 1.6	12.9 ± 1.6	15.8 ± 4.7	17.6 ± 3.8
	UC	49.3 ± 4.9	43.5 ± 6.2	10.2 ± 0.3	66.8 ± 4.4	46.7 ± 1.8	65.3 ± 3.3	69.4 ± 3.8	67.5 ± 0.5	62.0 ± 3.1	65.8 ± 3.8	74.3 ± 1.7	55.4 ± 11.1	55.8 ± 5.4	59.2 ± 1.0	55.8 ± 4.0	56.5 ± 2.0
	HC + UC (HUS)	18.5 ± 7.1	26.2 ± 15.7	11.9 ± 3.3	70.0 ± 3.0	49.2 ± 6.2	72.0 ± 2.9	77.7 ± 2.9	72.8 ± 1.0	70.2 ± 3.6	75.2 ± 1.8	84.2 ± 1.0	53.9 ± 9.4	62.9 ± 4.8	65.2 ± 2.3	66.3 ± 2.8	58.4 ± 0.5
	ESM	59.2 ± 2.2	62.0 ± 1.8	49.7 ± 4.0	84.3 ± 2.1	52.2 ± 2.3	83.3 ± 0.9	85.2 ± 0.8	78.3 ± 0.6	75.0 ± 0.6	85.2 ± 0.7	88.5 ± 0.3	78.8 ± 5.5	71.9 ± 2.0	71.8 ± 2.9	66.6 ± 2.3	72.8 ± 0.7
	HC + ESM	60.6 ± 3.2	64.7 ± 3.4	55.2 ± 7.7	84.8 ± 0.3	55.7 ± 8.8	82.1 ± 1.3	83.9 ± 1.7	81.8 ± 1.0	82.2 ± 1.7	83.6 ± 2.6	90.3 ± 0.9	82.5 ± 0.6	70.4 ± 5.5	76.6 ± 2.4	69.0 ± 6.1	74.9 ± 2.4
	UC + ESM	64.0 ± 1.9	67.7 ± 4.6	57.3 ± 2.9	84.2 ± 1.1	56.5 ± 3.5	84.5 ± 0.8	85.9 ± 0.7	78.7 ± 1.6	79.0 ± 1.1	85.1 ± 0.8	90.8 ± 0.4	84.9 ± 0.9	73.5 ± 1.0	76.8 ± 1.1	69.3 ± 1.9	75.9 ± 0.5
	HUS + ESM (SoTTA)	**73.3 ± 1.2**	**76.3 ± 1.9**	**66.3 ± 2.5**	**88.5 ± 0.6**	**68.3 ± 2.3**	**86.8 ± 0.7**	**88.3 ± 0.2**	**84.1 ± 1.0**	**84.2 ± 0.6**	**87.2 ± 0.4**	**92.0 ± 0.4**	**89.0 ± 1.1**	**77.8 ± 1.8**	**83.8 ± 0.9**	**77.8 ± 1.2**	**81.6 ± 0.6**
Attack	Source	26.0 ± 3.3	33.2 ± 3.5	24.7 ± 4.2	56.7 ± 2.7	52.0 ± 2.7	67.4 ± 1.2	64.8 ± 2.6	78.0 ± 0.4	67.0 ± 2.5	74.1 ± 0.8	91.5 ± 0.3	33.9 ± 1.8	76.6 ± 0.7	46.4 ± 0.6	73.2 ± 0.8	57.7 ± 1.0
	HC	10.2 ± 0.0	10.4 ± 0.3	10.1 ± 0.0	15.1 ± 7.0	11.7 ± 0.2	21.5 ± 4.4	31.6 ± 11.7	17.1 ± 3.5	13.1 ± 0.5	22.0 ± 6.7	32.6 ± 10.5	10.5 ± 0.3	18.5 ± 4.5	11.9 ± 0.5	17.2 ± 0.8	16.9 ± 1.6
	UC	44.1 ± 29.5	47.3 ± 32.3	10.1 ± 0.2	82.9 ± 1.4	63.1 ± 2.4	81.7 ± 1.5	84.8 ± 1.2	79.1 ± 1.8	79.0 ± 0.9	83.7 ± 1.0	88.3 ± 0.7	81.0 ± 0.8	73.2 ± 1.8	78.5 ± 3.8	73.3 ± 1.5	70.0 ± 3.9
	HC + UC (HUS)	16.1 ± 7.5	26.3 ± 23.9	10.3 ± 0.4	35.4 ± 19.3	42.1 ± 14.5	47.9 ± 14.7	54.4 ± 29.7	46.4 ± 14.4	45.3 ± 31.9	55.0 ± 24.3	49.8 ± 3.2	47.5 ± 27.0	42.6 ± 22.5	57.1 ± 11.6	36.5 ± 14.9	40.9 ± 5.5
	ESM	77.0 ± 0.6	79.5 ± 0.3	71.6 ± 0.4	89.0 ± 0.6	71.8 ± 0.6	88.3 ± 0.3	89.6 ± 0.6	86.3 ± 0.7	85.5 ± 0.6	88.1 ± 0.4	92.1 ± 0.0	87.2 ± 1.3	80.4 ± 0.8	85.4 ± 0.5	79.8 ± 0.9	83.4 ± 0.2
	HC + ESM	77.8 ± 0.3	79.7 ± 0.3	70.9 ± 0.2	89.3 ± 0.3	71.8 ± 1.4	87.9 ± 0.4	89.6 ± 0.5	86.1 ± 0.2	85.4 ± 0.3	88.7 ± 0.2	92.2 ± 0.1	87.3 ± 0.5	80.4 ± 0.6	85.7 ± 0.3	79.8 ± 0.6	83.5 ± 0.2
	UC + ESM	**78.2 ± 0.2**	80.1 ± 0.4	**72.3 ± 0.9**	89.9 ± 0.2	**73.6 ± 0.8**	89.1 ± 0.1	90.2 ± 0.2	86.7 ± 0.2	85.7 ± 0.2	**89.3 ± 0.3**	92.8 ± 0.1	**88.6 ± 0.2**	81.0 ± 0.8	86.0 ± 0.4	80.5 ± 0.5	84.3 ± 0.1
	HUS + ESM (SoTTA)	**78.2 ± 0.3**	**80.8 ± 0.1**	**72.3 ± 0.8**	**90.1 ± 0.2**	**73.6 ± 0.9**	**89.2 ± 0.4**	**90.3 ± 0.5**	**87.4 ± 0.5**	**86.2 ± 0.6**	**89.3 ± 0.6**	**92.9 ± 0.1**	87.8 ± 0.7	**81.3 ± 0.8**	**86.6 ± 0.3**	**81.0 ± 0.3**	**84.5 ± 0.2**
Noise	Source	26.0 ± 3.3	33.2 ± 3.5	24.7 ± 4.2	56.7 ± 2.7	52.0 ± 2.7	67.4 ± 1.2	64.8 ± 2.6	78.0 ± 0.4	67.0 ± 2.5	74.1 ± 0.8	**91.5 ± 0.3**	33.9 ± 1.8	76.6 ± 0.7	46.4 ± 0.6	73.2 ± 0.8	57.7 ± 1.0
	HC	10.3 ± 0.3	10.3 ± 0.1	10.1 ± 0.0	17.5 ± 9.5	11.8 ± 1.0	18.1 ± 3.7	18.9 ± 5.6	19.0 ± 1.3	14.1 ± 1.0	25.4 ± 10.9	41.6 ± 6.3	11.1 ± 1.5	15.1 ± 0.6	13.7 ± 0.6	14.6 ± 1.1	16.8 ± 0.2
	UC	24.8 ± 25.5	41.8 ± 27.4	10.1 ± 0.0	72.4 ± 3.4	53.0 ± 2.2	70.0 ± 1.5	74.1 ± 2.2	69.9 ± 2.1	69.9 ± 1.2	66.6 ± 10.0	77.9 ± 0.6	67.7 ± 1.9	64.2 ± 2.1	67.2 ± 1.1	63.2 ± 2.9	59.5 ± 3.0
	HC + UC (HUS)	21.7 ± 14.1	40.5 ± 19.4	10.7 ± 1.0	74.0 ± 4.6	46.6 ± 13.0	72.5 ± 4.1	78.1 ± 3.6	73.3 ± 0.9	71.3 ± 1.9	76.6 ± 2.3	81.1 ± 1.2	40.9 ± 17.3	65.9 ± 0.9	67.4 ± 2.7	63.3 ± 6.0	58.9 ± 2.6
	ESM	59.4 ± 2.1	59.9 ± 1.4	51.7 ± 1.5	62.0 ± 14.5	44.3 ± 7.0	57.1 ± 15.7	65.8 ± 5.7	65.8 ± 2.1	67.4 ± 3.7	60.9 ± 4.7	77.8 ± 2.6	56.2 ± 7.1	51.9 ± 4.3	63.8 ± 11.3	63.6 ± 6.3	60.5 ± 5.3
	HC + ESM	65.0 ± 2.0	68.2 ± 2.0	58.0 ± 3.2	74.8 ± 3.4	48.4 ± 4.2	67.6 ± 1.3	75.1 ± 2.8	71.4 ± 0.9	70.8 ± 4.0	74.0 ± 1.4	81.0 ± 0.2	70.8 ± 3.7	62.4 ± 2.3	72.9 ± 3.5	70.1 ± 2.3	68.7 ± 1.1
	UC + ESM	70.8 ± 4.7	75.9 ± 3.7	64.7 ± 2.9	83.4 ± 2.0	62.2 ± 2.1	82.2 ± 4.6	84.6 ± 0.9	81.2 ± 0.9	80.1 ± 1.2	82.6 ± 2.4	90.1 ± 1.1	79.8 ± 5.2	73.6 ± 3.6	77.7 ± 1.2	76.9 ± 1.0	77.7 ± 1.8
	HUS + ESM (SoTTA)	**73.3 ± 1.5**	**77.7 ± 0.8**	**66.8 ± 1.8**	**86.1 ± 2.1**	**64.0 ± 2.8**	**84.3 ± 0.7**	**86.6 ± 1.1**	**83.1 ± 0.7**	**82.0 ± 1.8**	**85.7 ± 2.7**	91.1 ± 0.4	**84.1 ± 2.4**	**77.1 ± 3.3**	**81.6 ± 2.8**	**77.2 ± 2.2**	**80.0 ± 1.4**

Table 9: Classification accuracy (%) and their corresponding standard deviations on ablation study of the size of Noise on CIFAR10-C for 15 types of corruptions. **Bold** numbers are the highest accuracy. Averaged over three different random seeds.

		Noise			Blur				Weather				Digital				
	Method	Gau.	Shot	Imp.	Def.	Gla.	Mot.	Zoom	Snow	Fro.	Fog	Brit.	Cont.	Elas.	Pix.	JPEG	Avg.
5000	Source	26.0 ± 3.3	33.2 ± 3.5	24.7 ± 4.2	56.7 ± 2.7	52.0 ± 2.7	67.4 ± 1.2	64.8 ± 2.6	78.0 ± 0.4	67.0 ± 2.5	74.1 ± 0.8	**91.5 ± 0.3**	33.9 ± 1.8	76.6 ± 0.7	46.4 ± 0.6	73.2 ± 0.8	57.7 ± 1.0
	BN stats [27]	59.6 ± 0.2	61.6 ± 0.7	51.5 ± 0.6	66.9 ± 1.2	49.8 ± 0.9	65.3 ± 0.1	68.6 ± 0.7	71.2 ± 0.5	71.5 ± 0.2	65.0 ± 0.6	84.2 ± 0.3	70.0 ± 1.1	58.8 ± 1.2	63.5 ± 0.5	65.4 ± 0.9	64.9 ± 0.4
	PL [17]	59.9 ± 4.7	61.3 ± 3.6	52.1 ± 1.7	66.4 ± 1.4	46.1 ± 4.2	62.7 ± 1.5	67.2 ± 2.7	69.6 ± 1.5	69.2 ± 1.3	65.4 ± 2.0	83.8 ± 1.2	66.8 ± 4.4	55.5 ± 3.0	64.9 ± 1.2	65.6 ± 4.3	63.8 ± 0.3
	TENT [38]	64.3 ± 2.0	70.0 ± 2.4	59.3 ± 0.1	68.8 ± 4.2	47.7 ± 3.1	65.8 ± 3.0	72.4 ± 4.9	73.6 ± 5.0	73.4 ± 5.3	65.4 ± 6.0	88.2 ± 0.8	69.0 ± 2.6	63.7 ± 3.8	72.2 ± 1.2	67.8 ± 5.6	68.1 ± 1.3
	LAME [1]	22.0 ± 3.6	28.9 ± 3.7	18.8 ± 3.5	52.2 ± 2.1	51.2 ± 3.5	64.9 ± 0.5	61.5 ± 1.4	78.9 ± 0.6	68.0 ± 4.1	72.3 ± 1.4	90.3 ± 0.3	27.6 ± 1.3	75.3 ± 0.7	43.6 ± 0.9	73.8 ± 1.0	55.3 ± 0.5
	CoTTA [39]	68.6 ± 1.5	69.7 ± 1.6	61.8 ± 1.8	64.9 ± 3.8	53.1 ± 4.0	62.1 ± 2.7	68.8 ± 2.0	72.6 ± 1.2	75.9 ± 0.4	64.5 ± 3.8	86.1 ± 0.3	62.1 ± 1.5	59.7 ± 2.8	71.0 ± 2.3	70.2 ± 1.7	67.4 ± 1.6
	EATA [28]	58.4 ± 0.3	61.7 ± 2.8	45.1 ± 6.5	58.8 ± 3.7	38.7 ± 9.3	57.9 ± 2.5	64.5 ± 3.9	62.7 ± 1.9	63.3 ± 3.3	62.2 ± 3.6	76.0 ± 0.7	54.6 ± 16.1	48.2 ± 2.9	64.6 ± 2.5	60.5 ± 1.7	58.5 ± 0.8
	SAR [29]	60.9 ± 1.3	63.0 ± 1.9	53.6 ± 2.5	67.5 ± 0.8	50.5 ± 0.4	65.9 ± 0.5	69.1 ± 0.4	71.2 ± 0.6	71.4 ± 0.2	65.4 ± 0.3	84.2 ± 0.3	70.3 ± 0.9	59.4 ± 0.7	63.7 ± 0.5	65.7 ± 0.6	65.5 ± 0.3
	RoTTA [44]	64.9 ± 0.5	67.0 ± 0.8	56.9 ± 1.2	81.4 ± 0.6	59.9 ± 0.9	81.1 ± 0.8	83.1 ± 0.4	80.1 ± 0.7	78.3 ± 1.1	78.9 ± 0.5	91.0 ± 0.4	68.0 ± 4.6	72.8 ± 0.7	73.9 ± 0.2	72.9 ± 0.9	74.0 ± 0.8
	SoTTA	**74.1 ± 1.0**	**77.3 ± 0.9**	**67.4 ± 0.2**	**86.2 ± 1.9**	**64.7 ± 2.5**	**85.0 ± 2.3**	**87.5 ± 1.1**	**84.3 ± 0.4**	**82.3 ± 1.0**	**85.0 ± 2.5**	91.4 ± 0.3	**83.5 ± 3.4**	**77.8 ± 2.2**	**82.7 ± 1.4**	**78.6 ± 0.9**	**80.5 ± 1.0**
10000	Source	26.0 ± 3.3	33.2 ± 3.5	24.7 ± 4.2	56.7 ± 2.7	52.0 ± 2.7	67.4 ± 1.2	64.8 ± 2.6	78.0 ± 0.4	67.0 ± 2.5	74.1 ± 0.8	**91.5 ± 0.3**	33.9 ± 1.8	76.6 ± 0.7	46.4 ± 0.6	73.2 ± 0.8	57.7 ± 1.0
	BN stats [27]	51.7 ± 0.3	53.9 ± 0.6	45.5 ± 0.7	52.7 ± 2.0	41.5 ± 1.7	51.0 ± 0.7	55.1 ± 1.5	62.8 ± 0.7	63.8 ± 0.2	53.8 ± 0.6	76.9 ± 0.3	55.8 ± 2.5	46.8 ± 1.8	54.8 ± 0.7	56.4 ± 1.0	54.8 ± 0.8
	PL [17]	47.6 ± 9.9	52.7 ± 2.4	44.7 ± 4.3	48.9 ± 12.6	36.1 ± 5.1	49.4 ± 1.8	54.1 ± 2.9	61.9 ± 2.4	56.5 ± 4.4	50.9 ± 1.3	77.1 ± 3.7	45.2 ± 4.8	43.1 ± 4.5	49.4 ± 5.6	59.5 ± 4.7	51.8 ± 0.9
	TENT [38]	54.0 ± 6.7	57.1 ± 5.6	36.7 ± 9.1	48.9 ± 6.8	28.3 ± 4.5	50.5 ± 3.1	51.0 ± 5.0	64.0 ± 4.1	64.7 ± 5.2	49.5 ± 1.9	80.5 ± 1.4	43.7 ± 3.0	38.4 ± 2.2	56.7 ± 6.4	57.0 ± 4.5	52.1 ± 0.4
	LAME [1]	21.8 ± 3.5	28.6 ± 3.7	18.5 ± 3.1	51.6 ± 2.3	50.8 ± 3.6	64.3 ± 0.2	60.9 ± 1.8	78.4 ± 0.5	67.3 ± 3.8	71.7 ± 1.2	90.5 ± 0.2	27.0 ± 1.2	75.1 ± 0.7	43.0 ± 0.9	73.4 ± 1.0	54.9 ± 0.6
	CoTTA [39]	60.4 ± 2.1	60.3 ± 3.5	52.4 ± 1.6	47.3 ± 3.0	41.6 ± 0.4	44.1 ± 2.7	52.0 ± 4.7	62.7 ± 0.6	66.6 ± 0.8	47.7 ± 2.4	79.0 ± 1.7	44.7 ± 1.1	42.8 ± 4.3	60.2 ± 0.5	60.2 ± 1.0	54.8 ± 1.3
	EATA [28]	42.2 ± 1.1	41.0 ± 1.1	33.2 ± 5.9	32.7 ± 5.1	25.0 ± 1.5	27.9 ± 2.1	34.3 ± 5.4	40.8 ± 2.7	42.6 ± 6.5	31.6 ± 11.5	61.5 ± 5.7	20.3 ± 2.2	27.5 ± 4.1	35.8 ± 4.5	43.1 ± 8.3	36.0 ± 0.8
	SAR [29]	57.5 ± 1.0	59.3 ± 0.2	49.6 ± 1.7	57.2 ± 1.1	43.7 ± 1.7	54.4 ± 1.5	59.4 ± 1.6	64.8 ± 1.0	65.4 ± 0.3	57.9 ± 0.4	77.1 ± 0.2	60.2 ± 1.8	50.0 ± 1.2	58.3 ± 0.6	59.8 ± 0.1	58.3 ± 0.3
	RoTTA [44]	64.4 ± 0.5	66.9 ± 0.8	56.1 ± 1.4	80.1 ± 0.4	59.1 ± 0.5	79.8 ± 0.2	82.2 ± 0.8	79.7 ± 0.8	78.7 ± 0.7	77.8 ± 0.4	91.2 ± 0.6	69.0 ± 4.0	72.3 ± 1.2	73.4 ± 0.2	72.8 ± 0.7	73.6 ± 0.5
	SoTTA	**73.3 ± 1.5**	**77.7 ± 0.8**	**66.8 ± 1.8**	**86.1 ± 2.1**	**64.0 ± 2.8**	**84.3 ± 0.7**	**86.6 ± 1.1**	**83.1 ± 0.7**	**82.0 ± 1.8**	**85.7 ± 2.7**	91.1 ± 0.4	**84.1 ± 2.4**	**77.1 ± 3.3**	**81.6 ± 2.8**	**77.2 ± 2.2**	**80.0 ± 1.4**
20000	Source	26.0 ± 3.3	33.2 ± 3.5	24.7 ± 4.2	56.7 ± 2.7	52.0 ± 2.7	67.4 ± 1.2	64.8 ± 2.6	78.0 ± 0.4	67.0 ± 2.5	74.1 ± 0.8	**91.5 ± 0.3**	33.9 ± 1.8	76.6 ± 0.7	46.4 ± 0.6	73.2 ± 0.8	57.7 ± 1.0
	BN stats [27]	41.3 ± 0.7	42.9 ± 1.0	37.2 ± 0.4	37.4 ± 2.1	32.6 ± 1.4	36.1 ± 1.0	39.6 ± 1.4	52.0 ± 0.7	52.7 ± 0.5	40.6 ± 1.2	65.0 ± 0.5	37.4 ± 4.1	33.9 ± 1.8	44.1 ± 0.9	44.4 ± 0.5	42.5 ± 0.8
	PL [17]	25.5 ± 1.1	22.6 ± 3.2	27.6 ± 4.2	20.5 ± 7.0	21.7 ± 5.0	20.2 ± 6.7	21.8 ± 1.4	50.0 ± 8.4	41.7 ± 13.4	24.0 ± 9.0	60.8 ± 8.3	17.7 ± 3.6	21.3 ± 9.2	23.1 ± 5.0	29.5 ± 10.1	28.5 ± 2.3
	TENT [38]	21.5 ± 4.5	19.7 ± 2.3	21.4 ± 2.2	14.2 ± 1.4	18.5 ± 3.4	17.8 ± 4.4	15.3 ± 3.5	44.2 ± 6.7	36.6 ± 4.8	15.2 ± 1.3	63.8 ± 5.2	19.9 ± 2.7	13.3 ± 1.8	28.1 ± 10.7	25.0 ± 8.3	25.0 ± 2.9
	LAME [1]	21.7 ± 3.4	28.2 ± 3.6	18.1 ± 3.0	50.4 ± 2.7	49.6 ± 3.0	63.6 ± 0.6	60.1 ± 2.0	77.9 ± 0.5	66.1 ± 3.3	71.0 ± 0.7	90.6 ± 0.1	26.6 ± 1.4	75.0 ± 0.5	42.6 ± 0.7	73.3 ± 0.7	54.3 ± 0.6
	CoTTA [39]	42.7 ± 1.5	46.7 ± 2.6	39.0 ± 3.0	31.0 ± 0.7	29.8 ± 2.2	32.0 ± 1.4	35.3 ± 2.4	50.9 ± 3.9	55.3 ± 3.5	31.9 ± 1.2	67.6 ± 1.2	28.9 ± 5.6	29.5 ± 3.2	45.9 ± 5.2	46.8 ± 2.8	40.9 ± 1.7
	EATA [28]	22.3 ± 3.8	23.9 ± 3.5	19.2 ± 1.1	15.1 ± 1.6	16.1 ± 4.6	15.9 ± 3.1	17.4 ± 2.3	21.8 ± 5.5	19.5 ± 0.9	15.1 ± 1.2	32.7 ± 9.4	14.7 ± 1.7	15.0 ± 2.0	20.9 ± 0.6	23.1 ± 2.9	19.5 ± 0.6
	SAR [29]	41.6 ± 1.9	43.7 ± 0.9	39.6 ± 2.6	33.4 ± 8.6	29.3 ± 5.4	34.6 ± 3.8	38.1 ± 3.2	55.8 ± 3.1	56.1 ± 3.0	38.5 ± 4.0	68.4 ± 3.2	33.0 ± 9.8	28.9 ± 7.2	46.6 ± 2.8	45.3 ± 0.8	42.2 ± 1.9
	RoTTA [44]	62.5 ± 0.5	64.5 ± 1.1	54.6 ± 1.7	78.9 ± 0.4	58.3 ± 0.4	79.0 ± 0.7	81.3 ± 1.0	80.0 ± 0.3	79.0 ± 0.4	77.3 ± 0.5	91.3 ± 0.4	69.0 ± 1.4	71.5 ± 0.8	73.4 ± 0.3	72.4 ± 0.6	72.9 ± 0.3
	SoTTA	**73.2 ± 1.0**	**75.6 ± 2.8**	**63.3 ± 3.8**	**83.2 ± 2.8**	**61.0 ± 3.5**	**84.5 ± 2.6**	**86.3 ± 2.4**	**82.6 ± 0.6**	**81.0 ± 3.3**	**84.8 ± 1.8**	89.7 ± 0.3	**82.8 ± 4.9**	**72.9 ± 2.4**	**81.1 ± 1.5**	**77.5 ± 1.0**	**78.6 ± 1.5**

C Additional ablative studies

We conducted experiments to understand the sensitivity of our two hyperparameters: confidence threshold (C_0) and BN momentum (m). We varied C_0 and m and reported the corresponding accuracy.

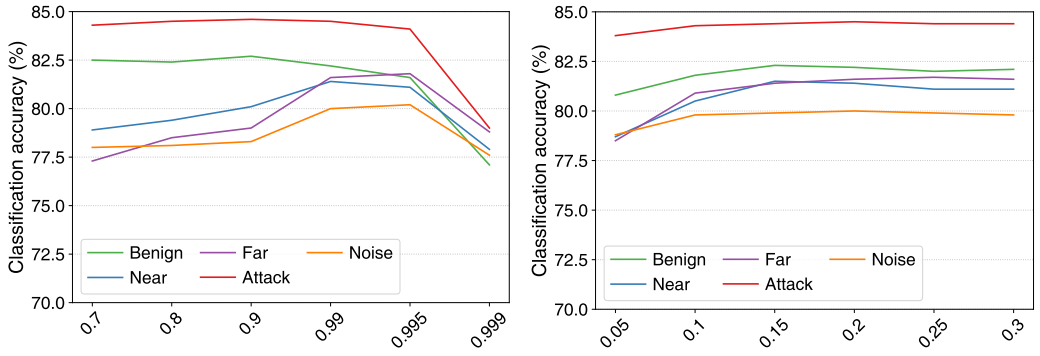

(a) Effect of hyperparameter C_0.

(b) Effect of hyperparameter m.

Figure 8: Effect of hyperparameters on the model accuracy on CIFAR10-C for 15 types of corruptions under five scenarios: Benign, Near, Far, Attack, and Noise. Averaged over three different random seeds.

Confidence threshold. Our result shows that the selection of C_0 shows similar patterns across different scenarios (Benign $\sim$ Noise). The result illustrates a tradeoff; a low C_0 value does not effectively reject noisy samples, while a high C_0 value filters benign data. We found a proper value of C_0 (0.99) that generally works well across the scenarios. Also, we found that the optimal C_0 depends primarily on in-distribution data. Our interpretation is that setting different C_0 values for CIFAR10-C, CIFAR100-C, and ImageNet-C is straightforward as they have a different number of classes (10, 100, and 1,000), which leads to different ranges of the model's confidence.

BN momentum. Across the tested range, the variations in performance were found to be negligible. This finding indicates that choosing a low momentum value from within the specified range ([0.05, 0.3]) is adequate to maintain a favorable performance. Please note that setting a high momentum would corrupt the result, which is implicated by the algorithms directly utilizing test-time statistics (e.g., TENT) suffering from accuracy degradation with noisy data streams (e.g., TENT: 81.0% $\rightarrow$ 52.1% for Noise at Table 1).

D Further discussions

D.1 Theoretical explanation of the impact of noisy data streams

We provide a theoretical explanation of the impact of noisy data streams with a common entropy minimization as an example. With the Bayesian-learning-based frameworks [2, 7], we can express the posterior distribution p of the model in terms of training data D and benign test data B in test-time adaptation:

$$\log p(\theta|D,B) = \log q(\theta) - \frac{\lambda_B}{|B|}\sum_{b=1}^{|B|} H(y_b|x_b). \tag{7}$$

The posterior distribution of model parameters depends on the prior distribution q and the average of entropy H of benign samples with a multiplier λ. Here, we incorporate the additional noisy data stream N into Equation 7 and introduce a new posterior distribution considering noisy streams:

$$\log p(\theta|D,B,N) = \log q(\theta) - \frac{\lambda_B}{|B|}\sum_{b=1}^{|B|} H(y_b|x_b) - \frac{\lambda_N}{|N|}\sum_{n=1}^{|N|} H(y_n|x_n). \tag{8}$$

Table 10: Average classification accuracy (%) and their corresponding standard deviations on ablation study of the effect of high-confidence uniform-class continual memory of SoTTA on CIFAR10-C. **Bold** numbers are the highest accuracy. Averaged over three different random seeds.

	Benign	Near	Far	Attack	Noise	Avg
SoTTA (w/o High-confidence)	82.2 ± 0.2	78.0 ± 0.4	75.9 ± 0.5	84.3 ± 0.1	77.7 ± 0.7	79.6 ± 0.2
SoTTA (w/o Uniform-class)	**82.3 ± 0.2**	80.9 ± 0.6	74.9 ± 2.4	83.5 ± 0.2	68.7 ± 7.0	78.0 ± 2.0
SoTTA (w/o Continual)	81.0 ± 0.5	79.5 ± 0.3	75.5 ± 1.8	84.4 ± 0.2	65.7 ± 7.0	77.2 ± 1.8
SoTTA	82.2 ± 0.3	**81.4 ± 0.5**	**81.6 ± 0.6**	**84.5 ± 0.2**	**80.0 ± 1.4**	**81.9 ± 0.5**

With Equation 7 and Equation 8, we can now derive model parameter variations caused by noisy test samples:

$$\log p(\theta|D,B) - \log p(\theta|D,B,N) = \frac{\lambda_N}{|N|}\sum_{n=1}^{M} H(y_n|x_n). \tag{9}$$

Equation 9 implies that the (1) model adapted only from benign data and (2) model adapted with both benign and noisy data differ by the amount of the average entropy of noisy samples. This also suggests that a high entropy from severe noisy samples would result in a significant model drift in adaptation (i.e., model corruption).

D.2 Comparison with previous TTA methods

D.2.1 EATA and SAR

While SoTTA, EATA [28], and SAR [29] all leverage sample filtering strategy, the key distinction of input-wise robustness of SoTTA and EATA/SAR lies in three aspects: (1) Our high-confidence sampling strategy in SoTTA aims to filter noisy samples by utilizing only the samples with high confidence, while both EATA and SAR use a different approach that excludes a few high-entropy samples, particularly during the early adaptation stage. In our preliminary study, we found that our method excludes 99.98% of the noisy samples, whereas EATA and SAR exclude 33.55% of such samples. (2) While EATA and SAR adapt to every incoming low-entropy sample, SoTTA leverages a uniform-class memory management approach to prevent overfitting. As shown in Figure 5b, noisy samples often lead to imbalanced class predictions, and these skewed distributions could lead to an undesirable bias in $p(y)$ and thus might negatively impact TTA objectives, such as entropy minimization. The ablation study in Table 10 shows the effectiveness of uniform sampling with a 3.9%p accuracy improvement. (3) EATA and SAR reset the memory buffer and restart the sample collection process for each adaptation. This strategy is susceptible to overfitting due to a smaller number of samples used for adaptation and the temporal distribution drift of the samples. In contrast, our continual memory management approach effectively mitigates this issue by retaining high-confidence uniform-class samples in the memory, as shown in Table 10.

We acknowledge that both SoTTA and SAR utilize sharpness-aware minimization proposed by Foret et al. [4]. However, we clarify that the motivation behind using SAM is different. While SAR intends to avoid model collapse when exposed to samples with large gradients, we aim to enhance the model's robustness to noisy samples with high confidence scores. As illustrated in Figure 6, we observed that entropy-sharpness minimization effectively prevents the model from overfitting to noisy samples. As a result, while our algorithm led to marginal performance degradation in noisy settings (82.2% $\rightarrow$ 80.0% for Noise), EATA and SAR showed significant degradation (EATA 82.4% $\rightarrow$ 36.0% for Noise; SAR 78.3% $\rightarrow$ 58.3% for Noise).

D.2.2 RoTTA

Regarding our high-confidence uniform sampling technique, RoTTA [44] could be compared. First of all, RoTTA's objective is different from ours; RoTTA focused on temporal distribution changes of test streams without considering noisy samples. Similar to SoTTA, RoTTA's memory bank maintains recent high-confidence samples. However, RoTTA has no filtering mechanism for low-confidence samples, which makes RoTTA fail to avoid noisy samples, especially in the early stage of TTA. In contrast, our confidence-based memory management scheme effectively rejects noisy samples, and

Table 11: Average classification accuracy (%) of ODIN+TTA on CIFAR10-C. **Bold** numbers are the accuracy with improvement from normal TTAs. Averaged over three different random seeds.

	Benign		Near		Far		Attack		Noise	
Method	w/o ODIN	w/ ODIN	w/o ODIN	w/ ODIN	w/o ODIN	w/ ODIN	w/o ODIN	w/ ODIN	w/o ODIN	w/ ODIN
Source	57.7 ± 1.0	57.7 ± 1.0	57.7 ± 1.0	57.7 ± 1.0	57.7 ± 1.0	57.7 ± 1.0	57.7 ± 1.0	57.7 ± 1.0	57.7 ± 1.0	57.7 ± 1.0
BN stats [27]	78.2 ± 0.3	78.2 ± 0.3	76.5 ± 0.4	76.5 ± 0.4	75.4 ± 0.3	**75.9** ± 0.4	55.8 ± 1.4	55.8 ± 1.4	55.9 ± 0.8	**56.7** ± 0.9
PL [17]	78.4 ± 0.3	**78.8** ± 0.5	73.1 ± 0.3	**74.3** ± 0.6	71.3 ± 1.0	**71.6** ± 0.8	66.5 ± 1.1	66.5 ± 1.1	52.1 ± 0.4	52.1 ± 0.4
TENT [38]	81.5 ± 1.0	81.5 ± 1.0	74.5 ± 0.8	**76.1** ± 0.6	73.5 ± 1.1	**74.7** ± 1.3	69.0 ± 0.9	**69.1** ± 1.0	54.4 ± 0.3	**56.2** ± 0.6
LAME [1]	56.1 ± 0.3	56.1 ± 0.3	56.7 ± 0.5	56.7 ± 0.5	55.7 ± 0.4	55.7 ± 0.4	56.2 ± 0.5	56.2 ± 0.5	54.9 ± 0.5	**55.2** ± 0.7
CoTTA [39]	82.2 ± 0.3	82.2 ± 0.3	78.2 ± 0.3	78.2 ± 0.4	73.6 ± 0.9	73.6 ± 0.9	69.6 ± 1.3	69.6 ± 1.3	57.8 ± 0.8	**62.0** ± 1.3
EATA [28]	82.4 ± 0.3	82.4 ± 0.3	63.9 ± 0.4	**69.2** ± 0.4	56.3 ± 0.5	**59.9** ± 0.6	70.9 ± 0.7	70.9 ± 0.7	36.0 ± 0.8	**50.8** ± 1.1
SAR [29]	78.4 ± 0.7	78.4 ± 0.7	72.8 ± 8.2	72.8 ± 8.2	75.7 ± 3.1	**76.0** ± 3.1	56.2 ± 1.8	56.2 ± 1.8	58.7 ± 0.3	58.7 ± 0.3
RoTTA [44]	75.3 ± 0.7	75.3 ± 0.7	77.5 ± 0.5	77.5 ± 0.5	77.0 ± 0.9	77.0 ± 0.9	78.4 ± 0.8	78.4 ± 0.8	73.5 ± 0.5	73.5 ± 0.5
SoTTA	82.1 ± 0.4	82.1 ± 0.4	81.6 ± 0.4	81.6 ± 0.4	81.7 ± 0.5	**82.0** ± 0.8	84.5 ± 0.3	84.5 ± 0.3	81.5 ± 1.2	81.5 ± 1.2

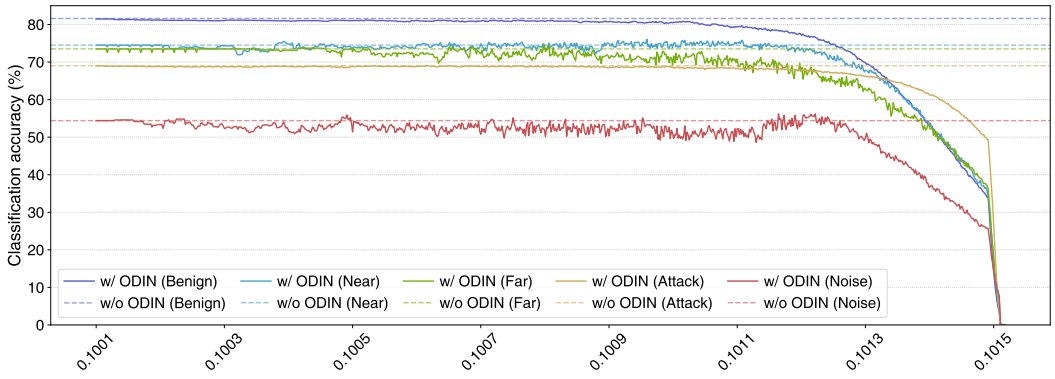

Figure 9: Effect of OOD threshold δ on classification accuracy (%) of ODIN+TENT on CIFAR10-C. Averaged over three different random seeds.

thus it prevents potential model drift from the beginning of TTA scenarios. As a result, our approach outperforms RoTTA in noisy test streams (e.g., 5.4%p better than RoTTA on CIFAR10-C).

D.3 Comparison with out-of-distribution detection algorithms

We discussed the limitation of applying out-of-distribution detection to TTA in Section 5. Still, we are curious about the effect of applying out-of-distribution algorithms to our scenario. To this end, we conduct experiments using one of the out-of-distribution algorithms, ODIN [20], in our noisy data streams. Specifically, we filtered OOD samples detected by ODIN and performed TTA algorithms on the samples left.

Note that similar to prior studies on OOD, ODIN uses a thresholding approach to predict whether a sample is OOD. It thus requires validation data with binary labels indicating whether it is in-distribution or OOD to decide the best threshold δ. However, in TTA scenarios, validation data is not provided, which makes it difficult to apply OOD algorithms directly in our scenario. We circumvented this problem using the labeled test batches to get the best threshold. Following the original paper, we searched for the best threshold from 0.1 to 0.12 with a step size of 0.000001, which took over 20,000 times longer than the original TTA algorithm.

Table 11 shows that the impact of discarding OOD samples with ODIN is negligible, yielding only a 0.3%p improvement in the average accuracy despite a huge computation cost. Also, Figure 9 shows the high sensitivity of ODIN with respect to threshold hyperparameter δ, which implies that applying OOD in TTA is impractical.

We conclude the practical limitations of OOD detection algorithms for TTA as follows: (1) OOD methods assume that a model is fixed during test time, while a model changes continually in TTA. (2) As previously noted, most OOD algorithms require labels for validation data unavailable in TTA scenarios. Even using the same test dataset for selecting the threshold, the performance improvement was marginal. (3) Low performance possibly results from the fact that OOD detection studies are

built on the condition that training and test domains are the same, which differs from TTA's scenario. These collectively make it difficult to apply OOD detection studies directly to TTA scenarios.

D.4 Applying to other domains

While this study primarily focuses on classification tasks, there are other tasks where test-time adaptation would be useful. Here we discuss the applicability of SoTTA to (1) image segmentation and (2) object detection, which are crucial in autonomous driving scenarios.

For image segmentation, when noisy objects are present in the input, the model might produce noisy predictions on those pixels, leading to detrimental results. Extending SoTTA to operate at the pixel level would allow it to be compatible with the segmentation task while minimizing the negative influences of those noisy pixels on model predictions in test-time adaptation scenarios.

Similarly, SoTTA could be tailored to object detection's classification (recognition) task. For example, in the context of the YOLO framework [32], SoTTA could filter and store grids with high confidence for test-time adaptation, enhancing detection accuracy. However, our current approach must address the localization task (bounding box regression) during test-time adaptation. Implementing this feature is non-trivial and would require careful consideration and potential redesign of certain aspects of our methodology. Accurately localizing bounding boxes during test-time adaptation presents an exciting avenue for future research.

E License of assets

Datasets CIFAR10/CIFAR100 (MIT License), CIFAR10-C/CIFAR100-C (Creative Commons Attribution 4.0 International), ImageNet-C (Apache 2.0), and MNIST (CC-BY-NC-SA 3.0).

Codes Torchvision for ResNet18 (Apache 2.0), the official repository of CoTTA (MIT License), the official repository of TENT (MIT License), the official repository of LAME (CC BY-NC-SA 4.0), the official repository of EATA (MIT License), the official repository of SAR (BSD 3-Clause License), and the official repository of RoTTA (MIT License).